RUNNING TITLE:

GIGANTEA and EEL regulate ABA synthesis

CORRESPONDING AUTHOR:

Dae-Jin Yun

Department of Biomedical Science & Engineering, Konkuk University, Seoul 05029, South Korea.

Tel: 02-450-0583. Email: djyun@konkuk.ac.kr

TITLE:

GIGANTEA and EEL interact to regulate diurnal ABA synthesis and the drought stress response

AUTHORS:

Dongwon Baek[1, †], Woe-Yeon Kim[1, 2, †], Joon-Yung Cha[1, 2], Hee Jin Park[3, 4], Gilok Shin[3], Junghoon Park[3], Chae Jin Lim[3], Hyun Jin Chun[2], Ning Li[5], Doh Hoon Kim[6], Sang Yeol Lee[1], Jose M. Pardo[7], Min Chul Kim[1], Dae-Jin Yun[3, 4, *]

AUTHORS/AFFILIATIONS:

[1] Division of Applied Life Science (BK21 PLUS), Plant Molecular Biology and Biotechnology Research Center, Gyeongsang National University, Jinju 52828, Korea,

[2] Institute of Agriculture & Life Science, Gyeongsang National University, Jinju 52828, Korea,

[3] Department of Biomedical Science and Engineering, Konkuk University, Seoul 05029, Korea,

[4] Institute of Glocal Disease Control, Konkuk University, Seoul 05029, Republic of Korea

[5] State Key Laboratory of Cultivation and Protection for Non-Wood Forest Trees, Ministry of Education, Central South University of Forestry and Technology, Changsha 410004, China

[6] College of Life Science and Natural Resources, Dong-A University, Busan 49315, Korea

[7] Instituto de Bioquímica Vegetal y Fotosíntesis, cicCartuja, CSIC-Universidad de Sevilla, AmericoVespucio 49, Sevilla 41092, Spain.

[†] These authors contributed equally to this work.

[*] Correspondence: Dae-Jin Yun (Email: djyun@konkuk.ac.kr), Tel: 02-450-0583

ONE-SENTENCE SUMMARY:

The GIGANTEA-EEL complex enhances plant tolerance to drought by modulating the diurnal transcription of *NCED3*, which encodes a rate-limiting enzyme in abscisic acid biosynthesis.

AUTHOR CONTRIBUTIONS

D.B., W.-Y.K., and D.-J.Y. designed the experiments and wrote the manuscript. D.B. performed most of the experiments. J.-Y.C. and H.J.P. helped to write the manuscript. G.S., J.M.P., C.J.L., M.S.C., H.J.C., and N.L. performed some of the experiments. D.H.K., S.Y.L., M.C.K., W.-Y.K., J.M.P. and D.-J.Y. discussed and commented on the results and revised the manuscript. All authors revised and approved the manuscript.

The author responsible for the distribution of materials integral to the findings presented in this article in accordance with the policy described in the Instructions for Authors (www.plantphysiol.org) is: Dae-Jin Yun (djyun@konkuk.ac.kr).

FUNDING

This study was supported by the Next Generation BioGreen21 Program (SSAC, grant numbers PJ01318201 to D.-J.Y., PJ01327301 to W.-Y.K, and PJ01318205 to J.M.P.), the Rural Development Administration Republic of Korea, and the Basic Science Research Program of the National Research Foundation of Korea (NRF), funded by the Ministry of Education (2016R1D1A1B01011803 to D.B., 2019R1A2C2084096 to D.-J.Y and Global Research Laboratory 2017K1A1A2013146 to D.-J.Y.).

KEYWORDS: *Arabidopsis thaliana*, drought stress, GIGANTEA (GI), ENHANCED EM LEVEL (EEL), 9-CIS-EPOXYCAROTENOID DIOXYGENASES 3 (NCED3), abscisic acid (ABA)

E-mail address of Author for Contact

Author Name	E-mail address
Dongwon Baek	atndpk@hotmail.com
Woe-Yeon Kim	kim1312@gnu.ac.kr
Joon-Yung Cha	jycha@gnu.ac.kr
Hee Jin Park	ckatowor@hotmail.com
Gilok Shin	newgolove@hanmail.net
Junghoon Park	p6259j@gmail.com
Chae Jin Lim	kirays2@nate.com
Hyun Jin Chun	hj_chun@hanmail.net
Ning Li	qtxsnning@hotmail.com
Doh Hoon Kim	dhkim@dau.ac.kr
Sang Yeol Lee	sylee@gnu.ac.kr
Jose M. Pardo	jose.pardo@csic.es
Min Chul Kim	mckim@gnu.ac.kr
Dae-Jin Yun	djyun@konkuk.ac.kr

ABSTRACT

Drought is one of the most critical environmental stresses limiting plant growth and crop productivity. The synthesis and signaling of abscisic acid (ABA), a key phytohormone in the drought stress response, is under photoperiodic control. GIGANTEA (GI), a key regulator of photoperiod-dependent flowering and the circadian rhythm, is also involved in the signaling pathways for various abiotic stresses. In this study, we isolated ENHANCED EM LEVEL (EEL)/bZIP12, a transcription factor involved in ABA signal responses, as a GI interactor. The diurnal expression of *9-CIS-EPOXYCAROTENOID DIOXYGENASE 3* (*NCED3*), a rate-limiting ABA biosynthetic enzyme, was reduced in the *eel*, *gi-1*, and *eel gi-1* mutants under regular growth conditions. ChIP and EMSA analyses revealed that EEL and GI bind directly to the ABA-Responsive Element (ABRE) motif in the *NCED3* promoter. Furthermore, the *eel*, *gi-1*, and *eel gi-1* mutants were hypersensitive to drought stress due to uncontrolled water loss. The transcript of *NCED3*, endogenous ABA levels and stomatal closure, were all reduced in the *eel*, *gi-1*, and *eel gi-1* mutants under drought stress. Our results suggest that the EEL-GI complex positively regulates the diurnal ABA synthesis by affecting the expression of *NCED3*, and contributes to the drought tolerance of *Arabidopsis*.

INTRODUCTION

The productivity and distribution of plants are adversely influenced by a variety of abiotic stresses, including drought, high salinity, and extreme temperatures (Zhu, 2016). Global climate change and the resulting water shortages are expected to escalate drought episodes, which would limit plant growth and development (Dai, 2013; Zhu, 2016). Plants have evolved distinct morphological and physiological adaptations that reduce the adverse impact of water shortages (Basu et al., 2016; Gilbert and Medina, 2016; Zhu, 2016). These adaptations are predominantly mediated by endogenous plant hormones, particularly abscisic acid (ABA) (Basu et al., 2016; Zhu, 2016). When the plant senses stress signals during periods of dehydration and osmotic stress, the endogenous ABA levels increase to promote stomatal closure, reducing the transpiration rate (Hirayama and Shinozaki, 2007; Cutler et al., 2010). ABA is not only involved in the response to various environmental challenges, including salinity, freezing, water deficit, wounding, and pathogen attack, but also plays a role in a wide range of developmental processes, such as seed germination, early seedling development, and reproduction (Finkelstein et al., 2002; Huang et al., 2008; Cutler et al., 2010; Cao et al., 2011; Hauser et al., 2011).

ABA-mediated signaling is activated or repressed through the regulation of several enzymatic reactions involved in its biosynthesis or degradation (Nambara and Marion-Poll, 2005; Dong et al., 2015; Chen et al., 2020). The first step of ABA biosynthesis takes place in plastids, where β-carotene is converted into xanthoxin, and the final step occurs in the cytosol (Seo and Koshiba, 2002). Epoxidation of all-trans-zeaxanthin is catalyzed to either 9-cis-violaxanthin or all-trans-neoxanthin by zeaxanthin epoxidase (ZEP) (Finkelstein, 2013). To produce xanthoxin, the oxidative cleavage by the 9-cis-epoxycarotenoid dioxygenases (NCEDs) is a key regulatory rate-limiting step in ABA biosynthesis following exposure to abiotic stresses (Iuchi et al., 2001; Qin and Zeevaart, 2002; Lefebvre et al., 2006; Martínez-Andújar et al., 2011). In *Arabidopsis thaliana*, the NCED family comprises five enzymes, NCED2, NCED3, NCED5, NCED6, and NCED9, which asymmetrically cleave carotenoids (Schwartz et al., 2003). Most NCED family members play individual regulatory roles in the responses to environmental stimuli and developmental processes (Iuchi et al., 2001; Tan et al., 2003). *NCED2* and *NCED3* are expressed during root development, while *NCED5*, *NCED6,* and *NCED9* are highly expressed in embryonic plants and induced during seed dormancy (Tan et al., 2003; Frey et al., 2012). *NCED3* is up-regulated upon exposure to drought and

high salt stress (Barrero et al., 2006; Endo et al., 2008; Hao et al., 2009), and has been shown to cooperate with *NCED5* to enhance stress-induced ABA synthesis (Frey et al., 2012). NCED6 is critical for ABA synthesis under photoreversible seed germination in Arabidopsis as the transcription of *NCED6* is induced upon exposure to far-red light (Seo et al., 2006). In addition, several transcription factors have been shown to regulate the *NCED*s under a variety of growth conditions (Jiang et al., 2012; Lee et al., 2015). WRKY57 induces the expression of *NCED3* and *RESPONSIVE TO DESICCATION 29A* (*RD29A*) by directly binding to the W-box in their promoters (Jiang et al., 2012). The transcription factor NGATHA1 (NGA1) regulates expression of *NCED3* by binding to NGA-binding element (NBE) (Sato et al., 2018), whereas HAT1 acts as a negative regulator by binding to the HB site within the *NCED3* promoter (Tan et al., 2018). Another transcription factor, MYB96, directly activates the transcription of *NCED2* and *NCED6* to modulate both ABA and gibberellin (GA) biosynthesis (Lee et al., 2015).

The levels of biologically active ABA are fine-tuned by ABA degradation and sugar-conjugation processes (Dietz et al., 2000; Xu et al., 2002; Kushiro et al., 2004; Saito et al., 2004). Sugar-conjugation represents a major pathway of ABA inactivation (Lee et al., 2006). Chemically modified and biologically inactive ABA can be recycled to rapidly increase the pool of the bioactive hormone. The β-glucosidase encoded by *Arabidopsis β-glucosidase 1* (*AtBG1*) hydrolyzes glucose-conjugated ABA into active ABA (Lee et al., 2006). The ABA release in de-conjugation processes by AtBG1 regulates both intra- and extracellular ABA levels, as well as gene expression in stress responses (Lee et al., 2006; Han et al., 2012). Mutation of *AtBG1* leads to reduced levels of bioactive ABA, the increase in stomata number and impaired stomatal closure in the drought stress response (Allen et al., 2019), whereas the overexpression enhances drought tolerance (Han et al., 2012). Among the catabolic pathways, ABA 8′-hydroxylation appears to be the regulatory step in a variety of physiological processes (Kushiro et al., 2004). The expression of genes encoding the ABA 8′-hydroxylases, *CYTOCHROME P450 FAMILY 707 SUBFAMILY A POLYPEPTIDE* (*CYP707A1*) and *CYP707A2*, is transiently induced after seed imbibition, but is rapidly down-regulated during seed germination (Saito et al., 2004; Okamoto et al., 2006).

The circadian clocks of plants anticipate environmental cues and synchronize physiological responses to occur at the most optimal time of the day. The metabolic pathways of phytohormones are under circadian regulation (Covington et al., 2008; Michael et al., 2008;

Grundy et al., 2015; Singh and Mas, 2018). The transcription of genes involved in the biosynthesis of auxin, salicylic acid (SA), jasmonic acid (JA), and ethylene (ET), as well as a large proportion of genes responsive to various abiotic stresses are rhythmically regulated (Yang et al., 2004; Covington and Harmer, 2007; Cheng et al., 2013; Wasternack and Hause, 2013; Kazan, 2015). For instance, the gene encoding the rate-limiting enzyme *ACC SYNTHASE 8* (*ACS8*) is rhythmically expressed for the circadian control of ET biosynthesis (Thain et al., 2004), while *ACS6* expression is rhythmically regulated by TOC1, a transcription factor playing as a core oscillator in the circadian clock (Grundy et al., 2015). TOC1 rhythmically regulates JA levels by binding to the promoter of the gene encoding the 13-lipoxyenase enzyme required for JA biosynthesis (Grundy et al., 2015). *PRR5* and *TOC1* also contribute to oscillations in SA levels by binding to the promoters of SA biosynthesis-related genes (Huang et al., 2012; Nakamichi et al., 2012; Liu et al., 2013). ABA biosynthesis and many ABA-responsive genes are under circadian control (Mizuno and Yamashino, 2008; Singh and Mas, 2018). In most species analyzed, including *A. thaliana* (Lee et al., 2006), the diurnal variations of ABA content reached a peak during daytime (Grundy et al., 2015; Adams et al., 2018). The diurnal changes of ABA abundance may be necessary for anticipating the diurnal day/night cycle in the regulation of stomata aperture, which in turn affects water consumption and the photosynthetic rate (Nováková et al., 2005; Mizuno and Yamashino, 2008; Grundy et al., 2015). Levels of bioactive ABA are principally regulated by the daily fluctuations of the *ABA1* and *NCED3* gene expression and by the polimerization-mediated activation of AtBG1 in the absence of stress (Lee et al., 2006; Fukushima et al., 2009). In tomato, *NCED1* showed a non-circadian diurnal accumulation during daytime (Thompson et al., 2000). The ABA-mediated stress response requires the key circadian clock regulators, CIRCADIAN CLOCK-ASSOCIATED1 (CCA1), LATE ELONGATED HYPOCOTYL (LHY), and TOC1 (Fukushima et al., 2009; Legnaioli et al., 2009; Adams et al., 2018). *TOC1* negatively regulates the circadian expression of the ABA receptors and the H subunit of the magnesium-protoporphyrin IX chelatase (*ABAR/CHLH/GUN5*) (Legnaioli et al., 2009). In addition, TOC1 coordinates drought tolerance and seed germination through its physical interaction with the PHYTOCHROME-INTERACTING FACTORs (PIFs), as well as with several ABA-related components such as DEHYDRATION-RESPONSIVE ELEMENT-BINDING 1A (DREB1A) and ABI3 (Kurup et al., 2000; Kidokoro et al., 2009; Kudo et al., 2017). Moreover, the interaction between *PIF7* and *TOC1* reduces the circadian

clock-associated expression of *DREB1C* during the drought stress response (Kidokoro et al., 2009). The function of LHY in ABA physiology is complex because LHY partly represses the diurnal expression of *NCED3* but at the same time promotes ABA responses, at least in part through the repression of phosphatases ABI1 and ABI2 (Adams et al., 2018).

GIGANTEA (GI) was originally isolated as a regulator of the photoperiodic flowering and the circadian clock (Koornnef et al., 1991; Fowler et al., 1999; Park et al., 1999; Mizoguchi et al., 2005). GI functions upstream of *CONSTANS* (*CO*), a floral activator that induces *FLOWERING LOCUS T* (*FT*) transcription in the circadian clock-controlled flowering pathway under long days (Koornneef et al., 1991; Suarez-Lopez et al., 2001). GI interacts with FLAVIN-BINDING KELCH REPEAT F-BOX 1 (FKF1), a blue light receptor F-box E3 ligase, in the afternoon in a light-dependent manner, and the resulting GI-FKF1 complex targets *CYCLING DOF FACTOR 1* (*CDF1*), a transcriptional repressor of *CO* (Imaizumi et al., 2005; Sawa et al., 2007). GI also plays diverse pleiotropic roles in various plant developmental processes, including light signaling, sugar metabolism, and cell wall deposition, as well as abiotic stress responses to oxidative stress, cold, drought, and salinity (Cao et al., 2007; Edwards et al., 2010; Dalchau et al., 2011; Kim et al., 2013; Riboni et al., 2013; Mishra and Panigrahi, 2015). In these responses, GI interacts with a wide range of partner proteins, such as ZEITLUPE (ZTL) for circadian clock regulation, FKF1 and CDF1 for flowering, SPINDLY (SPY) for light signaling, and SALT-OVERLY SENSITIVE 2 (SOS2) for the salt response (Tseng et al., 2004; Kim et al., 2007; Sawa et al., 2007; Kim et al., 2013). Most recently, GI has been found to promote floral induction via the activation of *FT* in response to ABA signaling (Riboni et al., 2016). Other components of the circadian clock have been found to be involved in the signal transduction that maintains hormonal balance in response to environmental stresses (Legnaioli et al., 2009; Seung et al., 2012; Lee et al., 2016).

Although GI forms one or more feedback loop(s) with the core clock oscillators to maintain the rhythmicity of the plant circadian clock (Fowler et al., 1999; Park et al., 1999; Swarup et al., 1999; Salomé et al., 2008), and has been shown to participate in various stress signaling pathways (Cao et al., 2005; Penfield and Hall, 2009; Kim et al., 2013; Han et al., 2013; Riboni et al., 2013), there are no reports linking the activity of GI to hormone synthesis. In this study, a yeast two-hybrid analysis revealed that ENHANCED EM LEVEL (EEL), a basic leucine zipper (bZIP) transcription factor involved in ABA-regulated gene expression

during seed dehydration, interacts with GI. The GI-EEL complex mediates drought tolerance by activating the diurnal expression of *NCED3* to up-regulate ABA biosynthesis. GI and EEL could therefore be targeted using molecular genetics to develop crop plants better able to withstand global climate changes.

RESULTS

GI interacts with EEL, a bZIP transcription factor

GI plays a role in the response to various abiotic stresses, such as high salinity, drought, and low temperatures (Cao et al., 2005; Penfield and Hall, 2009; Kim et al., 2013; Han et al., 2013; Riboni et al., 2013); however, the detailed molecular mechanism(s) by which GI contributes to the drought stress response remain largely unknown. We performed a mating-based yeast two-hybrid screen of an *Arabidopsis* cDNA library to identify proteins that interact with GI. First, the auto-activation of the reporter genes was tested using a full-length GI (GI^{full}) and truncated proteins ($GI^{1–749}$, $GI^{1–391}$, $GI^{543–1173}$, and $GI^{788–1173}$ amino acids) fused to the GAL4 DNA-binding domain (BD) of plasmid pGBK7 (Supplementary Figure S1A). The $GI^{543–1173}$ fragment was used for the yeast two-hybrid screen because it showed no auto-activation activity, while the GI^{full}, $GI^{1–749}$, $GI^{1–391}$, and $GI^{788–1173}$ proteins exhibited auto-activation in the absence of prey partners (Supplementary Figure S1B).

The yeast two-hybrid (Y2H) screening with $GI^{543–1173}$ revealed seven putative GI-interacting proteins (Supplementary Table S1). Among them, we selected EEL/AtbZIP12 (*At2g41070*) for further study because EEL (ENHANCED EM LEVEL) is a homolog of the bZIP transcription factor ABA-INSENSITIVE 5 (ABI5). ABI5 has critical roles in ABA signaling and ABA-dependent drought stress response (Kim et al., 2016). Moreover, EEL functions antagonistically with ABI5 to fine-tune the expression of LATE EMBRYOGENESIS–ABUNDANT (*LEA*) genes during seed maturation (Bensmihen et al., 2002). To confirm the interaction of the native GI with EEL in the Y2H system, we used next the *pDEST22* prey (AD) and *pDEST32* bait (BD) vector system (Figure 1A) (Park et al., 2018) in which full-length GI did not show auto-activation. In this assay, the full-length coding regions of GI and EEL were translationally fused to the *GAL4* transcription activation domain (GI-AD) and *GAL4* DNA-binding domain (EEL-BD), respectively. The yeast cells that were co-transformed with the GI-AD and EEL-BD constructs were able to grow on the synthetic complete medium lacking Trp, Leu, and His (SC-TLH) and containing 25 mM 3-AT, thus

confirming that GI physically interacted with EEL (Figure 1A). However, GI did not interact with ABI5, a close homolog of EEL (Supplementary Figure S2). The interaction of GI and EEL, we further confirmed by a co-immunoprecipitation (Co-IP) assay using total proteins from *Agrobacterium*-mediated tobacco (*Nicotiana benthamiana*) leaves after transient co-expression of GI and EEL (Figure 1B). Last, the interaction between GI and EEL *in vivo* was tested by a Bimolecular Fluorescence Complementation (BiFC) assay in *N. benthamiana* leaves. The full-length coding regions of *EEL* and *GI* cDNAs were fused with sequences encoding the N-terminal (^{VN}EEL or EEL^{VN}) and C-terminal fragments (^{VC}GI or GI^{VC}) of Venus (eYFP) fluorescent protein, respectively. Following the co-expression of ^{VN}EEL and ^{VC}GI or EEL^{VN} and GI^{VC} in tobacco leaves, reconstituted fluorescence signals were detected in the nuclei of the leaf epidermal cells (Figure 1C). Together, these data demonstrate that GI interacts specifically with the bZIP transcription factor EEL in the nucleus.

EEL and GI are involved in ABA biosynthesis

Clock components are essential for seed dormancy through their maintenance of hormonal balance, especially ABA and GA, and are known to affect ABA synthesis and signaling (Penfield and Hall, 2009; Grundy et al., 2015; Adams et al., 2018). Moreover, ABA levels show diurnal rhythms and peak 3-4 hours after dawn and before dusk in long-day photoperiod (Grundy et al., 2015; Adams et al., 2018). To determine whether EEL and GI affect the daily ABA metabolism, we examined the expression of genes encoding ABA biosynthesis enzymes in the single *eel*, *gi-1*, and double *eel gi-1* mutants. ABA DEFICIENT 1 (ABA1), ABA2, ABA3, and NCED3 are key regulators and rate-limiting enzymes of ABA biosynthesis. The qRT-PCR analysis revealed that the expression of *NCED3* at ZT4 (i.e. 4 h after dawn) was significantly down-regulated (ca. three-fold lower) in the *eel*, *gi-1*, and *eel gi-1* mutants in comparison with WT under normal growth conditions (Figure 2A). In contrast, the expression levels of *ABA1* and *ABA2* were similar in both WT and the mutants (Figure 2A). Unexpectedly, *ABA3* showed reduced expression relative to the WT only in *eel* mutant, but not the *gi-1* or the double mutant (Figure 2A). Importantly, we found that *NCED3* transcripts accumulated gradually during daytime and declined sharply at night, and that this photoperiodic transcription required both EEL and GI (Figure 2A). This result led us to check the transcriptional changes of the other *NCED* family genes in the *eel*, *gi-1*, and *eel gi-1* mutants. The expression of *NCED5* was halved in the *eel gi-1* double mutant compared with

WT, but no statistically significant change in *NCED5* expression was observed in the *eel* and *gi-1* single mutants (Supplementary Figure S3). The expression patterns of the other *NCED* genes did not differ in any of the genotypes tested (Supplementary Figure S3). These results suggest that EEL and GI positively co-regulate the diurnal expression of *NCED3* and *NCED5*, although the later gene was observed only in the *eel gi-1* double mutant.

Because *NCED3* expression showed GI-dependent diurnal oscillations and NCED3 function is linked to ABA synthesis (Iuchi et al., 2001), we determined the ABA content in WT, *gi-1* and GI-overexpressing (*GI-OX*) seedlings at ZT4, which coincides with the reported diurnal maxima of non-stress ABA in LDs (Grundy et al., 2015), and ZT12 when the *NCED3* expression was maximal (Figure 2B). Results showed that the ABA content in seedlings of the *gi-1* mutant was significantly reduced relative to the WT in equal conditions (Figure 2C). By contrast, GI overexpression had no effect on ABA accumulation at ZT4 and produced a modest increase at ZT12 relative to the WT. These results indicate that the diurnal accumulation of endogenous ABA is positively regulated by the GI protein, most likely through the regulation of *NCED3* transcription. Although the *gi-1* mutant showed some degree of stress-induced ABA synthesis, the total ABA produced under dehydration stress was reduced in the *gi-1* seedlings compared to the wild-type. The commensurate reduction of ABA content in the *gi-1* mutant before and after dehydration suggests that GI is less relevant for the enhanced ABA synthesis elicited by dehydration, which could still be observed in the *gi-1* mutant, than for the diurnal production of ABA.

The GI-EEL complex activates *NCED3* expression through binding to the promoter of *NCED3*

Several transcription factors are involved in regulating the expression of ABA biosynthesis-related genes to maintain ABA homeostasis (Jiang et al., 2012; Lee et al., 2015). Among them, ATAF1, a NAC transcription factor, transcriptionally regulates *NCED3* by binding to the non-ABRE consensus binding site *TTGCGTA* (Jensen et al., 2013). To determine whether GI and EEL regulate the transcription of *NCED3* directly or indirectly, we examined the physical interaction of the EEL and GI proteins with the promoter of *NCED3 in planta*. We performed a chromatin immunoprecipitation (ChIP) assay with HA-tagged *GI*-overexpressing (*GI*-OX) and myc-tagged *EEL*-overexpressing (*EEL*-OX) transgenic plants. For this, the *NCED3* promoter was divided into six different regions to design amplicons used for ChIP (Figure

3A). Significantly more amplicon 5 (P5) was precipitated in the *GI*-OX and *EEL*-OX plants than in the WT (Figure 3B and 3C), suggesting that GI and EEL regulate *NCED3* expression by binding to the P5 region in the *NCED3* promoter. An *in silico* analysis demonstrated that amplicon P5 contains a *cis*-acting ABRE (*CACGTGGC*) regulatory element with a consensus G-box (*CACGTG*) (Figure 4A). EEL is known to function by directly binding to the ABRE motif in the promoter of *LATE EMBRYOGENESIS ABUNDANT1* (*EM1*) (Bensmihen et al., 2002). To determine whether EEL can directly bind to the putative ABRE motif in the *NCED3* promoter, we performed an electrophoretic mobility shift assay (EMSA) using EEL fused to glutathione S-transferase (GST) produced in *E. coli*. The EEL recombinant protein bound the ABRE motif in the *NCED3* promoter (Figure 4B). To analyze the specificity of this *cis*-motif-binding activity, we added unlabeled core probes as inhibitors in the EMSA. The non-labeled oligonucleotides containing the ABRE motif competed with the labeled ABRE probe and reduced their binding to EEL-GST proportionately with the concentration of unlabeled probes added (Figure 4B). These results indicate that EEL directly binds to the ABRE motif on the promoter of *NCED3*.

To examine how GI and EEL regulate the transcription of *NCED3*, transient expression assays were performed using *Arabidopsis* protoplasts. To make the reporter construct, the promoter region of *NCED3* was transcriptionally fused to the upstream region of the β-glucuronidase (*GUS*) gene. In addition, constructs encoding GFP-tagged GI and myc-tagged EEL were generated as effector constructs, both under the control of the *CaMV 35S* promoter (Figure 5A). The luciferase (*LUC*) gene under the control of the *CaMV 35S* promoter was used for signal readout normalization. The reporter and effector plasmids were co-transformed into the protoplasts, and the GUS and LUC activities were measured. Both of the GI-GFP and EEL-myc proteins activated the *NCED3* promoter-driven GUS activity. Co-transformation with the *GI-GFP* and *EEL-myc* effectors had an additive effect on the trans-activation of the reporter compared to *EEL-myc* alone (Figure 5B). These results were further supported by transient expression of non-tagged GI and EEL proteins in tobacco leaves using the *NCED3:GUS* construct as the reporter (Figure 5C). Together, these results indicate that both EEL and GI are able to activate *NCED3* transcription.

EEL and GI enhance plant tolerance under drought stress condition

GI has multiple functions in various plant environmental responses, especially drought and

saline stresses (Riboni et al., 2013; Han et al., 2013; Kim et al., 2013; Riboni et al., 2016). By contrast, EEL participates in ABA-regulated gene expression during seeds dehydration but has no known role on water-stressed plants (Bensmihen et al., 2002). To characterize the functions of EEL and GI in the drought stress response, the loss-of-function *eel* and *gi-1* mutants and overexpressing transgenic plants were exposed to drought conditions for 11 days, followed by one day of re-watering. After re-watering, *eel* and *gi-1* mutants showed 9.52% and 15.48% of survival rate compared to more than 60% of WT (Figure 6A and 6C). A different mutant allele, *gi-2*, also showed the hypersensitive phenotype to drought stress (Supplementary Figure S4). However, the overexpression of *EEL* (*EEL*-OX; 71.43%) and *GI* (*GI*-OX; 69.05%) enhanced only weakly the tolerance of these plants to drought stress in comparison with WT (Figure 6A and 6C). Drought stress leads to dehydration because the water lost by transpiration is not replaced. The transpiration rate is therefore used as a physiological parameter associated to the drought tolerance or sensitivity of plants (Basu et al., 2016). To measure the rate of water loss under dehydration stress, rosette leaves of the *eel*, *gi-1* mutants, *EEL*-OX, *GI*-OX and WT plants were detached, and their fresh weights were measured over a two-hour period (Figure 6B and 6D). The detached leaves of the *eel* and *gi-1* mutants lost water more rapidly than WT, and *EEL*-OX and *GI*-OX genotypes decreased the water loss only marginally (Figure 6B and 6D). The hypersensitivity of *eel* and *gi* mutants to drought stress suggested that both EEL and GI positively regulate the drought response.

To specifically characterize the function of the EEL-GI complex in the drought stress response, the *eel gi-1* double mutants were also exposed to drought conditions for nine days, followed by one day of re-watering, together with the single *eel* and *gi-1* mutants used as parents. Survival of the double mutants was only marginally worse than that of the single mutants, indicating that the simultaneous loss of EEL and GI proteins had no additive effects and they likely work in the same process (Figure 7A). To measure the rate of water loss under drought stress, rosette leaves of the two-independent *eel gi-1* mutants and WT plants were detached, and their fresh weights were measured over a two-hour period (Figure 7B). The detached leaves of the *eel gi-1* double mutant plants lost much more water than the WT but again they did not depart from the phenotype of the single mutants (Figure 7B).

EEL and GI contribute towards ABA homeostasis and stomatal closure in the drought stress response

NCED3 expression is induced by water deficit, and has been associated with plant tolerance during drought stress (Iuchi et al., 2001). To investigate whether EEL and GI affect the transcription of *NCED3* during drought stress condition, 10-day-old seedlings of WT, *eel*, *gi-1*, and *eel gi-1* mutants were dehydrated for different time points (0 to 60 min) on petri-dishes. The results of qRT-PCR analysis indicated that *NCED3* expression was rapidly induced in the WT, but it was much less up-regulated during dehydration in the mutant plants compared to WT (Figure 8A). Time-course leaf ABA contents were also measured to examine whether EEL and GI affected dehydration-induced ABA levels. ABA accumulation in the *eel*, *gi-1*, and *eel gi-1* mutants was significantly lower than in the WT plants under both normal and dehydration conditions and similar to those resulting from the loss of NCED3 activity (Figure 8B).

Drought stress induces stomatal closure (Sirichandra et al., 2009). To investigate whether EEL and GI influence drought stress-mediated changes in stomatal physiology, the stomatal patterning and closure responses were determined in the *eel*, *gi-1*, and *eel gi-1* mutants. The stomatal density and guard cell sizes were similar in leaves of all genotypes at the same developmental stage (Figure 8C). The stomatal apertures were also similar in leaves floated on stomata-opening buffer. However, when leaves were exposed to dehydrating conditions, the stomata of the *eel*, *gi-1*, and *eel gi-1* mutants closed much less than those of the WT (Figure 8C and 8D). Together, these results indicated that the impaired stomatal closure of the *eel*, *gi-1*, and *eel gi-1* mutants was mainly caused by their low levels of stress-induced ABA. Therefore, EEL and GI enhance the plant tolerance by regulating ABA homeostasis and stomatal closure in the drought stress response.

DISCUSSION

Various abiotic stresses, such as heat, cold, salinity, and dehydration, affect the circadian expression of stress-responsive genes (Covington et al., 2008; Singh and Mas, 2018). The expression of genes involved in biosynthesis of the phytohormone ABA and regulating drought stress response is under control of circadian clock (Nambara and Marion-Poll, 2005; Agarwal and Jha, 2010; Basu et al., 2016; Adams et al. 2018). However, how ABA is rhythmically accumulated through diurnal biosynthesis remains poorly understood. In Arabidopsis, the endogenous ABA level peaks during the day (Grundy et al., 2015; Adams et al., 2018), in agreement with our observation of the diurnal expression pattern of *NCED3* (Figure 2). Circadian clock components such as PSEUDO-RESPONSE REGULATOR 5 (PRR5), PRR7, and TIMING OF CAB EXPRESSION 1 (TOC1), are indirectly involved in the increase of the ABA levels, whereas LHY functions to repress *NCED3* and ABA synthesis (Nakamichi et al., 2010; Huang et al., 2012; Liu et al., 2013; Adams et al., 2018). Here, we have shown that GI, a clock component involved in the regulation of circadian rhythms and photoperiodic flowering, makes a complex with the bZIP transcription factor EEL to regulate the expression of *NCED3*, the gene encoding a key rate limiting enzyme in ABA synthesis. *NCED3* showed a diurnal oscillation in which the transcript accumulated during daytime and declined at night (Figure 2). The expression during daytime was strictly dependent on GI and EEL (Figure 2). Indeed, *NCED3* expression recapitulates the diurnal pattern of GI protein abundance (Yu et al., 2008), suggesting that GI activity contributes towards the circadian amplitude of *NCED3* expression and ABA oscillations. This is consistent with the known role of GI in gating the light input into the photoperiodic pathway of flowering (Imaizumi et al., 2005; Sawa et al., 2007). GI is not a DNA-binding protein *per se* but influences gene expression through the interaction with DNA-finding transcription factors that recruit GI to specific gene promoters (Imaizumi et al., 2005; Sawa et al., 2007; Fornara et al., 2009; Kubota et al., 2017). Here, we show that GI and EEL interact to target the *NCED3* gene promoter to gate the light information that dictates the diurnal oscillations of *NCED3* and endogenous ABA synthesis. We suggest that EEL provides the target specificity for the *NCED3* promoter and that GI cooperates with EEL in gating the light input in the transcriptional regulation of *NCED3*.

NCED3 expression is also highly responsive to dehydration and contributes to the stress-induced ABA synthesis (Iuchi et al., 2001), and the abundance of *NCED3* transcripts

and ABA contents were reduced in the *gi* and *eel* mutants under dehydrating conditions (Figure 8). The overall reduction in ABA content in the *gi-1* and *eel* mutants correlated with the dehydration-sensitive phenotype (Figure 8). However, the *gi-1* and *eel* mutants retained some ability to induce *NCED3* expression and ABA synthesis upon dehydration treatment, in agreement with the known regulation of *NCED3* by additional factors (Jiang et al., 2012; Sato et al., 2018; Tan et al., 2018; Adams et al., 2018). Together, these results imply that the EEL-GI complex is principally required for the regulation of the diurnal fluctuations of ABA contents by gating the light input while contributing to the amplification of the dehydration signal.

GI regulation of ABA metabolism and stress responses

ABA is generally considered to be a floral repressor, in contrast to GAs that are flowering accelerators (Blazquez et al., 1998; Conti et al., 2014). Exogenous ABA treatment inhibits flowering by reducing the expression of *FT*, a floral integrator (Blazquez et al., 1998; Domagalska et al., 2010), while endogenous ABA promotes flowering via the upregulation of *FT*, as part of the drought response (Riboni et al., 2013). Short-term drought or water shortage promotes the floral transition as a drought-escape (DE) response via the upregulation of *FT* to avoid prolonged exposure to drought (Riboni et al., 2013). The DE response does not occur under short-day conditions or in the *gi* mutant, indicating that DE requires GI and the expression of its downstream targets *FT* and *SUPPRESSOR OF OVEREXPRESSION OF CONSTANS 1* (*SOC1*) (Riboni et al., 2013). These observations all suggest that there is a molecular crosstalk between ABA signaling and the photoperiodic pathway to flowering.

Several regulatory components of the circadian rhythm are involved in the regulation of the signaling pathways of diverse stresses (Franks et al., 2007; Legnaioli et al., 2009; Penfield and Hall, 2009). GI, a key regulator of the photoperiodic flowering and the circadian clock, also plays important roles in the responses to various stresses, including cold, drought, salt, and oxidative stress (Kurepa et al., 1998; Cao et al., 2005; Riboni et al., 2013; Kim et al., 2013). GI is a negative regulator in salt stress signaling via the inhibitory interaction with the SOS2 protein kinase that is essential for the activation of the Na^+/H^+ antiporter SOS1 (Quintero et al., 2011; Kim et al., 2013). Salinity promoted the proteasomal degradation of GI, with the subsequent release of SOS2 and the activation of SOS1 (Kim et al., 2013). The SOS

pathway is primarily involved in counteracting sodicity stress, independently of the water stress imposed by high salinity, and is considered an ABA-independent response (Xiong et al., 2002; Ji et al., 2013). Therefore, although salt and drought stresses both enhance the levels of the endogenous ABA and *NCED3* expression, GI could have different functions in the salt and drought stress responses. Firstly, *gi* mutants show enhanced salt-tolerance but are hypersensitive to drought stress and lack the early flowering liked to the drought escape response (Han et al., 2013; Riboni et al., 2013). This could indicate that GI protein integrity must be preserved under drought stress because GI must accumulate to promote flowering. Prior research had shown that GI is involved in the drought stress response, but the underlying mechanism was not fully understood except that GI interacted with miRNA172 to regulate the expression of the gene encoding the WRKY44 transcription factor (Han et al., 2013). Here we show that GI, together with EEL, promoted the diurnal expression of *NCED3* and mediated stomatal closure in the drought stress response (Figure 8C and 8D). Although the clock components PRR5, PRR7 and TOC1 are also involved in the control of stomatal aperture and expression of ABA responsive genes, how these clock elements regulate the rhythmicity of ABA biosynthesis remains largely unknown (Grundy et al., 2015). Together, these findings suggest that core clock components are intimately associated with plant responses to abiotic stresses.

Our results reveal that GI interacts with a bZIP transcription factor, EEL (Figure 1), and that the GI-EEL complex binds to the *NCED3* promoter region containing an ABRE to induce its expression for de novo ABA biosynthesis (Figures 2, 3, 4 and 8). *NCED5*, but none of the other *NCED*s (*NCED2*, *6* and *9*), appear to be influenced by the GI-EEL complex (Supplementary Figure S3). This is coherent with the know role of *NCED5* to enhance stress-induced ABA synthesis in addition to *NCED3* (Frey et al., 2012). The results of the transcriptional activation of the *NCED3* promoter by GI and EEL proteins using *Arabidopsis* protoplast and tobacco agro-infiltration systems (Figure 5) suggest that GI and EEL act as positive effectors in a transcriptional activator complex. The GI protein interacts with other transcription factors in the photoperiodic flowering pathway, such as CYCLING DOF FACTOR 1(CDF1), FLOWERING BHLH (FBH), FLAVIN BINDING KELCH REPEAT F-BOX 1 (FKF1), TEOSINTE BRANCHED 1/ CYCLOIDEA/ PROLIFERATING CELL NUCLEAR ANTIGEN FACTOR 4 (TCP4) (Imaizumi et al., 2005; Sawa et al., 2007; Fornara et al., 2009; Kubota et al., 2017). Although GI formed complexes with these transcription

493 factors to modulate their activity, GI did not bind directly to the DNA of target genes
494 (Imaizumi et al., 2005; Sawa et al., 2007; Fornara et al., 2009; Kubota et al., 2017). The
495 expression pattern of *NCED3* under long-day condition is similar to the steady accumulation
496 of the GI protein during daytime (Yu et al., 2008). Thus, *NCED3* expression was induced
497 when the *GI* expression was started at ZT4, and remained constant thereafter. The rhythmical
498 fluctuations of ABA are also known to be regulated by the PRR5, 7, and 9 clock components
499 (Fukushima et al., 2009). Loss-of-function mutant of LHY showed an altered rhythmical
500 accumulation of ABA, with a reduction of ABA content at dusk (Adams et al., 2018). It has
501 been suggested that LHY may repress light-dependent *NCED3* expression (Adams et al.,
502 2018). Together, our data show that GI and EEL stimulate diurnal ABA biosynthesis and plant
503 drought tolerance by up-regulating the transcriptional expression of *NCED3*, but whether the
504 EEL-GI complex operates to relieve inhibition by LHY is presently unknown.
505
506 **A novel role for EEL in ABA biosynthesis during drought stress**
507 The bZIP transcription factors in *Arabidopsis* are reported to regulate the expression of genes
508 involved in various abiotic stress responses (Yang et al., 2009; Alves et al., 2013; Kim et al.,
509 2015). The bZIP family includes 75 distinct members classified into 13 groups (A to L, and S)
510 according to their sequence similarity and functions (Kim, 2006). Group A genes are involved
511 in ABA signaling, and are divided into two categories, the ABI5/AtDPBF family members
512 (*ABI5*, *EEL*, *DPBF2/AtbZIP67*, *DPBF4*, and *AREB3*) and AREB/ABF family members
513 (*AREB1/ABF2*, *AREB2/ABF4*, *ABF1*, and *ABF3*) (Choi et al., 2000; Bensmihen et al., 2005;
514 Fujita et al., 2005). The ABI5/AtDPBF family members, including EEL, transcriptionally
515 regulate systems mediating ABA-dependent stress signaling during seed maturation and
516 developmental processes (Finkelstein and Lynch, 2000; Bensmihen et al., 2005). Accordingly,
517 *EEL* is strongly expressed in seeds, where EEL functions as either a homodimer or in a
518 heterodimer complex with ABI5 to interact with the *cis*-acting regulatory element ABRE of
519 genes such as *EM1* and *EM6*, during embryo maturation (Bensmihen et al., 2002; Carles et al.,
520 2002). However, *EEL* is also expressed in other plant tissues at lower levels (TAIR,
521 https://www.arabidopsis.org/), and our qRT-PCR analysis showed the presence of *EEL*
522 transcripts in vegetative tissues, including root, rosette leaves, cauline leaves, stem and
523 flowers, although the levels were low (Supplementary Figure S5). Moreover, EEL regulated
524 the expression of *STAYGREEN1* (*SGR1*) in the chlorophyll degradation pathway during leaf

senescence (Sakuraba et al., 2016). ABI5, which shows a preferential expression in seeds like EEL, was also involved in several abiotic stress responses of whole plants, such as drought, salt and high temperature (Lim et al., 2013; Song et al., 2013; Skubacz et al., 2016; Chang et al., 2019). Here we show that the loss-of-function mutant *eel* exhibited drought hypersensitivity (Figures 6A and 7A), and was found to contain lower levels of endogenous and stress-induced ABA (Figure 8B), and faster water loss upon dehydration than the WT (Figure 6B and 7B). In addition, the significant decrease of *NCED3* expression in the *eel* mutant indicates that EEL positively controls ABA biosynthesis by acting as a transcriptional activator of *NCED3* (Figure 2 and 8A). Although the *NCED3* promoter contains two putative ABRE *cis*-acting regulatory elements (Supplementary Figure S6) (Baek et al., 2017), EEL was associated only with the ABRE site in the P5 region of the *NCED3* promoter in our EMSA and ChIP experiments (Figures 3 and 4). Although EEL and ABI5 can associate as either homodimers or heterodimers (Bensmihen et al., 2002), we observed that ABI5 was not able to bind to the ABRE on the *NCED3* promoter, suggesting that only EEL induces *NCED3* expression specifically (Supplementary Figure S7). Apart from EEL, other transcription factors contribute to regulate *NCED3* expression according to various consensus binding sites and conditions. For example, ATAF1, a NAC transcription factor, regulates *NCED3* transcription by binding to the non-ABRE consensus binding site TTGCGTA (Jensen et al., 2013), i.e., AtAF1 and EEL transcription factors use different binding sites in the *NCED3* promoter. In addition, AtAF1 is related to plant growth and flowering time, whereas EEL is involved in seed germination and, as we show here, the dehydration stress response of seedlings and mature plants. Although most *NCED* family members have a few putative ABRE and/or ABRE-like *cis*-acting regulatory elements on their promoters, the expression levels of these other genes do not seem to be largely affected by EEL indicating that EEL regulates *NCED3* specifically.

CONCLUSIONS

In summary, we have shown that the GI-EEL complex regulates the diurnal oscillation of ABA biosynthesis by means of the transcriptional activation of *NCED3*. Overall ABA contents after dehydration stress were also reduced in *eel*, *gi-1*, and *eel gi-1* mutants, which were all hypersensitive to drought stress. In addition, GI and EEL act together to regulate stomatal closure. Plants regularly experience basal levels of water deficiency by

evapotranspiration on a daily basis, and circadian clock-controlled ABA biosynthesis and the resulting stomatal closure after dawn, are essential preemptive measures for maintaining water homeostasis. This study shows that GI, a circadian clock component and flowering time regulator, is also essential for plant acclimation to daily water demands by elevating the amount of endogenous ABA in cooperation with the transcription factor EEL. Collectively, the interdependence of ABA signaling and the circadian clock highlights an adaptive strategy to deal with recurrent daily strains and adverse environments.

MATERIALS AND METHODS

Yeast Two-Hybrid Screen and Interaction Assay

To identify GI-interacting proteins, a yeast two-hybrid screen was performed using the Matchmaker^{TM} Gold Yeast Two-Hybrid System (Takara Bio, Kusatsu, Japan), which is based on the mating of two haploid yeast strains that independently express the bait and prey fusion proteins. The full-length and truncated *GI* sequences were amplified using PCR and cloned into the pGBK7 bait vector (Supplementary Figure S1A). These constructs were transformed into *Saccharomyces cerevisiae* Y187 strain used in the yeast mating protocol. Only the truncated protein GI$^{543–1173}$ fragment could be used for the yeast two-hybrid screen because it showed no auto-activation activity. To confirm the protein-protein interactions found in the library screen, the full-length *GI* or *EEL* sequences were cloned into the pDEST22 prey vector (GI-AD) or pDEST32 bait vector (EEL-BD) and co-transformed into the yeast cells (Figure 1A) (Park et al., 2018). Of note is that full-length GI did not show auto-activation in this alternative Y2H system. Protein-protein interactions were determined by the growth of yeast colonies on the synthetic complete (Sc) medium lacking Trp and Leu (Sc-TL) or Trp, Leu and His (Sc-TLH; Takara Bio, Kusatsu, Japan) agar media containing X-gal (40 μg/mL) or 3-amino-1,2,4-triazole (3-AT; 25 mM).

Co-immunoprecipitation Assays

The leaves of three-week-old *Nicotiana benthamiana* plants were co-infiltrated with *Agrobacterium tumefaciens* carrying *35S:GI-GFP* and *35S:myc-EEL* together with the *p19* plasmid (Park et al., 2018). Total proteins extracted from co-infiltrated leaves and reacted for immunoprecipitation using anti-myc antibody (Roche, Indianapolis, IN, USA) and protein A agarose (Invitrogen, Carlsbad, CA, USA). For immunoblotting, membranes were incubated

589 with the appropriate anti-GFP (Abcam, Cambridge, MA, USA), and detected using ECL-
590 detection reagent (GE Healthcare, Little Chalfont, Buckinghamshire, UK). The co-
591 immunoprecipitation assays were performed in three independent replicates.
592
593 **Bimolecular Fluorescence Complementation (BiFC) Assay**
594 To confirm the protein-protein interaction *in vivo*, a BiFC assay was performed (Tian et al.,
595 2011). The full-length *EEL* or *GI* sequences were cloned into the binary BiFC-gateway
596 vectors, *pDEST-VYNE(R)*^{GW} or *pDEST-VYCE(R)*^{GW} or *pDEST-* ^{GW}*VYNE* or *pDEST-* ^{GW}*VYCE*
597 (Gehl et al., 2009). The leaves of four-week-old *Nicotiana benthamiana* plants were co-
598 infiltrated with *Agrobacterium tumefaciens* carrying *pDEST-VYNE(R)*^{GW}*-EEL* (^{VN}*EEL*) or
599 *pDEST-VYCE(R)*^{GW}*-GI* (^{VC}*GI*) or *pDEST-*^{GW}*VYNE-EEL* (*EEL*^{VN}) or *pDEST-*^{GW}*VYCE-GI* (*GI*^{VC})
600 together with the *p19* plasmid in infiltration buffer (10 mM MES, 10 mM $MgCl_2$, 100 µM
601 acetosyringone) at OD_{600}=0.5. After two days of incubation, the fluorescence signals were
602 detected using a confocal laser scanning microscope (Olympus FV1000; Tokyo, Japan) with a
603 GFP filter (excitation, 485 nm; emission, 535 nm) (Baek et al., 2019).
604
605 **Plant Materials and Growth Conditions**
606 The *Arabidopsis eel* mutant (SALK_021965), *gi-1* mutant, and *CaMV 35S* promoter *GI-OX*
607 transgenic plants (ecotype Col-0; Kim et al., 2007) were used in this study. The *eel gi-1* doble
608 mutants were generated by crossing *gi-1* with *eel*, and then isolated in the F2 progeny by
609 diagnostic PCR. Plants were grown on 1/2 x Murashige and Skoog (MS) media [1.5% (w/v)
610 sucrose, 0.6% (w/v) agar, pH 5.7] at 23°C. For the germination assay, the seeds were sown on
611 a 1/2 x MS agar medium supplemented with different concentrations of ABA, and five-day-
612 old seedlings with green cotyledons were scored as resistant to ABA inhibition. For the
613 drought treatments, water was withheld from 3-week-old plants for nine days, and their
614 survival ratio was measured on the 10^{th} day after one day of re-watering. The drought
615 experiments were performed for five independent replicates, each using at least 12 plants.
616
617 **Quantitative Real-Time PCR Analysis**
618 Total RNA was isolated from 10-day-old seedlings using an RNeasy Kit (Qiagen, Hilden,
619 Germany) following the manufacturer's instructions. The RNA was treated with DNase I
620 (Qiagen, Hilden, Germany) to remove contamination from genomic DNA. For the qRT-PCR

analysis, the first-strand cDNA was synthesized from 1 μg of total RNA using a cDNA synthesis kit (Thermo Fisher Scientific, Waltham, MA, USA). The QuantiSpeed SYBR No-Rox Mix (PhileKorea, Seoul, Republic of Korea) was used for the qRT-PCR reactions as follows: 50°C for 10 min, 95°C for 2 min, and 50 cycles of 95°C for 5 s and 60°C for 30 s. *TUBULIN2* expression was used for normalization. The relative expression levels of all samples were automatically calculated from three biological replicates using the CFX Manager software program (Bio-Rad Laboratories, Hercules, CA, USA). The qRT-PCR analyses were performed in three biological replicates, each with three technical replicates. The primers used for the qRT-PCR analyses were listed in Supplementary Table S2.

Generation of Transgenic Plants

To generate *EEL*-overexpressing transgenic plants, the full-length cDNA of the *EEL* gene was inserted into the *pGWB17* vector (with myc tag) under the control of the constitutive *CaMV 35S* promoter using the gateway system (Nakagawa et al., 2007; Ali et al., 2018). The primers used in the PCR are listed in Supplementary Table S2. The construct was introduced into *Agrobacterium tumefaciens* GV3101, then transformed into the wild-type plants by floral dipping. Transgenic plants were selected for hygromycin resistance and their genotypes were confirmed using RT-PCR. The homologous T_3 generation plants were used for further experiments.

Chromatin Immunoprecipitation (ChIP) Assay

The ChIP assays were performed as described by Saleh et al. (2008) using nuclear proteins extracted from the leaves (100 mg) of three-week-old WT, *EEL* (fused myc tag)-overexpressing, and *GI* (fused GFP tag)-overexpressing plants. Monoclonal anti-myc (Cell Signaling Technology, Denvers, MA, USA) or monoclonal anti-GFP (Thermo Fisher Scientific, Waltham, MA, USA) antibodies were used for the immunoprecipitation. The amount of immunoprecipitated DNA was quantified using qRT-PCR. The ChIP assays were performed in three independent replicates. The primers used in the ChIP assays were listed in Supplementary Table S2.

Electrophoretic Mobility Shift Assay (EMSA)

The EMSA was performed using the Lightshift Chemiluminescent EMSA kit (Thermo Fisher

Scientific, Waltham, MA, USA) according to the manufacturer's instructions (Yang et al., 2018). The probes were labeled with the 3' end biotin (Cosmo Genetech, Seoul, Republic of Korea), oligonucleotides spanning the ABRE binding site motif on the *NCED3* promoter. The DNA binding took place in a 20 min reaction at 25°C in binding buffer (10 mM Tris pH 7.5, 50 mM KCl, 1 mM dithiothreitol) containing 50 mM KCl, 0.05% (w/v) NP-40, 5 mM $MgCl_2$, 10 mM EDTA, 2.5% (w/v) glycerol, 50 ng/μL of poly (dI-dC), and various concentrations of purified bacterially expressed GST-EEL protein. For the competition assay, 2-, 5-, and 10-fold amounts of unlabeled probe were incubated with the GST-EEL protein before the labeled probe was added to the reaction. The reaction mixture was subjected to electrophoresis on a 6% (w/v) polyacrylamide gel in 0.5 x TBE buffer at 100 V for 2 h, transferred onto a nylon membrane, and then cross-linked. The biotin-labeled DNA was detected using chemiluminescence (Thermo Fisher Scientific, Waltham, MA, USA). The EMSA experiments were performed in three independent replicates.

Analysis of Transcriptional Activity

The plasmids indicated in the figure legends were introduced into protoplasts obtained from three-week-old *Arabidopsis* WT plants using PEG-mediated transformation (Baek et al., 2013). The expression of the fusion constructs was monitored and imaged using a Zeiss Axioplan fluorescence microscope (Carl Zeiss, Oberkochen, Germany), and the transcriptional activity of the EEL or GI proteins was analyzed in the protoplasts as described previously (Baek et al., 2013). The fluorescence was measured using a SpectraMax GEMINI XPS spectrofluorometer (Molecular Devices, San Jose, CA, USA) and SoftMax Pro-5 software (Molecular Devices, San Jose, CA, USA). The β-glucuronidase (GUS) activity was normalized to the LUC activity to eliminate experimental variation between samples. Each experiment was replicated three-independent times.

Gravimetric Water Loss Assay

The shoots of four-week-old plants were detached from the root and weighed immediately. The shoots were placed on a plate at room temperature and weighed at various time intervals. The loss of fresh weight was calculated as a percentage of the initial weight of the plant. At least five biological replicates were performed for each sample.

Stomatal Aperture Assays

Three or four leaves of 10-day-old seedlings were detached and floated on stomatal opening buffer (5 mM MES, 5 mM KCl, 50 μM $CaCl_2$, pH 5.6) under light conditions for 3 h. And then, to treat drought stress, leaves samples treated with dehydration for 1 h using filter paper for air dry. After drought stress treatment, the leaves were sequentially fixed by 2.5% glutaraldehyde and 1% OsO_4 in the dark condition. Images of stomata were captured by scanning electron microscopy (JSM-6380LV; JEOL, Akishima, Japan). The stomatal aperture was determined from measurements of 40 to 60 stomata per treatment. Each experiment was replicated three times.

Measurement of ABA Content

Endogenous ABA was extracted from 10-day-old seedlings (100 mg) and analyzed using a Phytodetek ABA test kit (Agdia Inc., Elkhart, IN, USA), following the manufacturer's protocols. At least three biological repeats and two technical repeats were performed for each sample.

Statistical Analyses

The statistical analyses including Student's t test were performed by using the Excel 2010 program. The quantitative real-time PCR (qRT-PCR) analyses were performed three-independent experiments the average values of $2^{\Delta CT}$ were used to determine the differences, and the data indicated as means ± SD. A significant difference was considered at $0.01 < \text{p-value} \leq 0.05$ and p-value ≤ 0.01. Where indicated analysis of variance by one-way ANOVA (MS Excel software) with Tukey test of significance for each experiments (p-value ≤ 0.05) was applied.

ACKNOWLEDGMENTS

We thank Professor Yong-Hwan Moon (Pusan National University) for providing the seeds of the *nced3* mutant.

SUPPLEMENTARY INFORMATION

Supplementary Figures

Supplementary Figure S1. Auto-activation between the GI protein and the GAL4 activation

domain (AD) in the Matchmaker yeast two-hybrid screen system.

Supplementary Figure S2. Yeast-two-hybrid assay of GI and ABI5 proteins.

Supplementary Figure S3. The expression of *NCED* family genes in WT plants, *eel*, *gi-1*, and *eel gi-1* mutants.

Supplementary Figure S4. Characterization of the drought stress responses of the *gi-2* mutant.

Supplementary Figure S5. The expression of *NCED3*, *GI* and *EEL* in various tissues of *Arabidopsis thaliana*.

Supplementary Figure S6. Putative ABRE *cis*-acting regulatory elements in the promoters of the *NCED* family.

Supplementary Figure S7. EMSA using ABI5 and the ABRE binding site motif in the *NCED3* promoter.

Supplementary Tables

Supplementary Table S1. Summary of GI-interacting proteins revealed in a yeast two-hybrid screen

Supplementary Table S2. List of primers used in this study

FIGURE LEGENDS

Figure 1. Interaction between the GI and EEL proteins.

(A) Protein-protein interaction assay using a yeast two-hybrid system. Prey is the *pDEST22* plasmid with the AD domain of GAL4, and Bait is the *pDEST32* plasmid with BD domain. Yeast cells co-transformed with GI-AD and EEL-BD were plated on the control SC-TL and selective medium SC-TLH with 25 mM 3-AT. The combinations with empty vector plasmids were used as negative controls. (B) Co-immunprecipitation assay with EEL and GI proteins. Total proteins extracted from *Nicotiana benthamiana* leaves co-infiltrated with GI-GFP and myc-EEL constructs. Input levels of epitope tagged proteins in total protein extracts were analyzed by immunoblotting with anti-myc and anti-GFP antibodies. Immunoprecipitated myc-tagged proteins were probed with anti-GFP antibody to detect co-immunoprecipitation of GI-GFP with myc-EEL. (C) GI and EEL interaction using BiFC assays in tobacco cells. The VN and VC represent the N- and C- terminal domain of Venus (eYFP), respectively. The GI-EEL complex was localized to the nucleus of the tobacco leaf epidermal cells. Plasmid combinations of ^{VN}EEL and ^{VC}GI (Upper) or EEL^{VN} and GI^{VC} (Bottom) are indicated above the images. The combinations with empty vector plasmids were used as negative controls. Scale bars represented 100 μm.

Figure 2. The diurnal expression of the ABA biosynthesis-related gene *NCED3* requires EEL and GI.

(A) Transcript levels of *NCED3*, *ABA1*, *ABA2*, and *ABA3* in WT plants, *eel*, *gi-1*, and *eel gi-1* mutants. The 10-day-old seedlings grown on 1/2 MS medium under long-day cycles were sampled 4 hours after dawn (ZT4) and submitted to total RNA extraction. The transcript levels of *NCED3*, *ABA1*, *ABA2* and *ABA3* were measured using qRT-PCR. The *TUBULIN2* was used as an internal control for normalization. Error bars represent the SD from three biological replicates, each with three technical replicates. Asterisks represent significant differences from the WT (**, p-value $\leq$ 0.01, Student's t-test). (B) Transcript levels of *NCED3* were analyzed in WT plants and *gi-1* or *eel* mutants grown on 1/2 MS medium for 10 days under a long-day photoperiod. Transcript levels were measured using qRT-PCR from total RNA extracted from seedlings at different ZT times. The white and black bars below the plot indicate the light and darkness periods, respectively. *TUBULIN2* was used as an internal

control for normalization. Error bars represent the SD from three biological replicates, each with three technical replicates. Asterisks represent significant differences from WT (*, 0.01 < *p*-value ≤ 0.05, **, *p*-value ≤ 0.01, Student's *t*-test). (C) ABA content in 10-day-old seedlings of wild-type (WT), *gi-1* and *GI*-OX plants grown on 1/2 MS medium under long-day cycles and sampled 4 and 12 hours after dawn (ZT4 and ZT12). ABA contents were measured from 20 whole seedlings of each genotype. Error bars represent the SD from three biological replicates, each with three technical replicates. Different letters indicate significantly different values at p-value ≤ 0.05 determined by one-way ANOVA.

Figure 3. EEL and GI associate with the *NCED3* promoter *in vivo*.

(A) Schematic drawing of the *NCED3* locus and locations of the ChIP assay amplicons (P1 to P6). The 1,000 bp upstream of the transcription start site on the *NCED3* genes was used. (B, C) The ChIP assay of the *NCED3* chromatin regions associated with GI and EEL. The ChIP assays were performed on nuclear proteins extracted from 10-day-old seedling of wild-type (WT) and those of *GI*-OX (B) or *EEL*-OX (C) seedlings. Plants were grown on 1/2 x MS under long-day conditions. Samples were prepared for the ChIP analysis using an anti-HA (B) or anti-myc antibody (C). The immunoprecipitated DNA was amplified using qRT-PCR with specific primers for the amplicons. The *TUBULIN2* was used as an internal control for normalization. The fold enrichment is the ratio of *GI*-OX or *EEL*-OX to WT signal. N.D. means not detected. Error bars represent the SD from three biological replicates, each with three technical replicates. Asterisks represent significant differences from the WT (**, *p*-value ≤ 0.01, Student's *t*-test).

Figure 4. EEL bind to the *NCED3* promoter.

(A) Schematic drawing of the ABRE binding site motif locus and sequence in the *NCED3* promoter. (B) The EMSAs were conducted using the GST-EEL fusion protein. The probe containing the ABRE binding site motif was biotin-labeled for use in the reaction. Unlabeled probes were also included in the reaction as competitors in the specified ratios to the biotin-labeled probe. The arrow indicates the EEL protein and ABRE probe complex.

Figure 5. Transcriptional activity assay of GI and EEL.

(A) A schematic representation of the effector and reporter constructs used in the transient

799 expression assay. (B) Protoplasts were isolated from the leaves of 3-week-old *Arabidopsis*
800 plants, and were co-transfected with the reporter plasmids NCED3:GUS and 35S:LUC, and
801 with one of the effector plasmids (empy vector-GFP, GI-GFP, empty vector-myc, and EEL-
802 myc). The *35S:LUC* plasmid was used for signal normalization. The GUS reporter activity in
803 each sample combination is presented as the GUS/LUC ratio. (C) The *NCED3* promoter was
804 fused to *GUS* and co-expressed in tobacco leaves together with different combinations of
805 EEL and GI. The images of GUS staining in the top panels show leaves expressing the
806 indicated constructs. The middle panel presents the quantification of GUS activity. The
807 bottom panel shows transcript levels of *GI*, *EEL*, or *GUS* in infiltrated tobacco leaves
808 quantified using RT-PCR. Tobacco *18S rRNA* expression was detected as a loading control.
809 Error bars represent the SD from three independent experiments. Different letters indicate
810 significantly different values at p-value $\leq$ 0.05 determined by one-way ANOVA.

811

812 **Figure 6. Characterization of the drought responses of the *eel* and *gi-1* mutants.**
813 Drought stress response of wild-type (WT), *eel*, and *EEL*-OX (A, B) or *gi-1* and *GI*-OX (C, D)
814 plants. The plants were grown in soil with sufficient water for two weeks (upper panel in A
815 and C), then water was withheld for 9 days (middle panels in A and C). The drought stress
816 was then alleviated by re-watering the plants for one day (bottom panels in A and C). The
817 survival rates of the plants were determined from three replicates, each of which involved at
818 least 12 plants. (B, D) Water loss by transpiration was measured from detached leaves of
819 four-week-old WT, *eel*, and *EEL*-OX (B) or *gi-1*, and *GI*-OX (D) plants. The water loss at
820 each time point was calculated as a percentage of the initial fresh weight (n=10). Error bars
821 represent the SD from three independent experiments. Asterisks represent significant
822 differences from the WT (*, 0.01 < p-value $\leq$ 0.05; **, p-value $\leq$ 0.01, Student's t-test).

823

824 **Figure 7. Characterization of the drought stress responses of the *eel gi-1* double mutants.**
825 (A) Wild-type (WT) plants, and *eel*, *gi-1*, and *eel gi-1* mutants were grown in soil with
826 sufficient water for three weeks (upper panels), then water was withheld for nine days
827 (middle panels). The drought-stressed plants were then re-watered for one day (bottom panel),
828 after which their survival rates were assessed. Each experiment comprised at least 12 plants,
829 and three replicates were performed. (B) Water loss by transpiration was measured from the
830 leaves of WT plants, *eel*, *gi-1*, and *eel gi-1* mutants. The shoots of three-week-old plants were

detached and their water loss at each time point was calculated as a percentage of their initial fresh weight (*n*=10). Error bars represent SD from three independent experiments. Asterisks represent significant differences from the WT (*, 0.01 < *p*-value ≤ 0.05; **, p-value ≤ 0.01, Student's *t*-test).

Figure 8. The expression of *NCED3*, ABA levels and stomatal closure in WT plants, the *eel*, *gi-1*, and *eel gi-1* mutants under drought stress condition.

(A) Transcript levels of *NCED3* in wild-type (WT) plants, and of *eel*, *gi-1*, and *eel gi-1* mutants over 1-hour dehydration stress. Ten-day-old seedlings grown on 1/2 MS medium under long-day cycles were sampled at ZT4 (control non-treated sample) and again 30 and 60 minutes after a dehydration treatment. *NCED3* transcript levels were measured using qRT-PCR. The expression of *TUBULIN2* was used as an internal control for normalization. Error bars represent the SD of three biological replicates, each with three technical replicates. (B) ABA content in seedlings treated as in (A). ABA contents were measured from 20 whole seedlings of each genotype. Error bars represent the SD from four independent experiments. (C) The rosette leaf epidermis of WT plants, *eel*, *gi-1* and *eel gi-1* mutants were floated in stomatal opening solution for 2 h, and then removed and placed onto filter paper for 1h for the dehydration treatment. Stomata on the abaxial surface were observed using scanning electron microscopy. Scale bar indicates 10 μm. (D) Measurement of stomatal apertures (width/length) in WT plants, *eel*, *gi-1* and *eel gi-1* mutants before and after dehydration for 1h. Error bars represent the SD from three independent experiments, with at least 30 stomata measured per genotype and per treatment. Asterisks represent significant differences from the WT (*, 0.01 < *p*-value ≤ 0.05; **, p-value ≤ 0.01, Student's *t*-test).

REFERENCES

Adams S, Grundy J, Veflingstad SR, Dyer NP, Hannah MA, Ott S, Carré IA. (2018) Circadian control of abscisic acid biosynthesis and signalling pathways revealed by genome-wide analysis of LHY binding targets. New Phytol. 220(3):893-907.

Agarwal PK, Jha B. (2010) Transcription factors in plants and ABA dependent and independent abiotic stress signalling. Biol.Plant. 54(2):201–212.

Ali A, Khan IU, Jan M, Khan HA, Hussain S, Nisar M, Chung WS, Yun DJ. (2018) The High-Affinity Potassium Transporter EpHKT1;2 From the Extremophile Eutrema parvula Mediates Salt Tolerance. Front Plant Sci. 9:1108.

Allen J, Guo K, Zhang D, Ince M, Jammes F. (2019) A-glucose ester hydrolyzing enzyme ATBG1 and PHYB antagonistically regulate stomatal development. PLoS One. 14(6):e0218605.

Alves MS, Dadalto SP, Gonçalves AB, De Souza GB, Barros VA, Fietto LG. (2013) Plant bZIP transcription factors responsive to pathogens: a review. Int J Mol Sci. 14(4):7815-7828.

Baek D, Chun HJ, Yun DJ, Kim MC. (2017) Cross-talk between Phosphate Starvation and Other Environmental Stress Signaling Pathways in Plants. Mol Cells. 40(10):697-705.

Baek D, Kim MC, Chun HJ, Kang S, Park HC, Shin G, Park J, Shen M, Hong H, Kim WY, Kim DH, Lee SY, Bressan RA, Bohnert HJ, Yun DJ. (2013) Regulation of miR399f transcription by AtMYB2 affects phosphate starvation responses in Arabidopsis. Plant Physiol. 161(1):362-373.

Baek D, Kim MC, Kumar D, Park B, Cheong MS, Choi W, Park HC, Chun HJ, Park HJ, Lee SY, Bressan RA, Kim JY, Yun DJ. (2019) AtPR5K2, a PR5-Like Receptor Kinase, Modulates Plant Responses to Drought Stress by Phosphorylating Protein Phosphatase 2Cs. Front Plant Sci. 10:1146.

Barrero JM, Rodríguez PL, Quesada V, Piqueras P, Ponce MR, Micol JL. (2006) Both abscisic acid (ABA)-dependent and ABA-independent pathways govern the induction of NCED3, AAO3 and ABA1 in response to salt stress. Plant Cell Environ. 29(10):2000-2008.

Basu S, Ramegowda V, Kumar A, Pereira A. (2016) Plant adaptation to drought stress. F1000Res. 5. pii: F1000 Faculty Rev-1554.

Bensmihen S, Giraudat J, Parcy F. (2005) Characterization of three homologous basic leucine

887 zipper transcription factors (bZIP) of the ABI5 family during Arabidopsis thaliana
888 embryo maturation. J Exp Bot. 56(412):597-603.
889 Bensmihen S, Rippa S, Lambert G, Jublot D, Pautot V, Granier F, Giraudat J, Parcy F. (2002)
890 The homologous ABI5 and EEL transcription factors function antagonistically to fine-
891 tune gene expression during late embryogenesis. Plant Cell. 14(6):1391-1403.
892 Blazquez MA, Green R, Nilsson O, Sussman MR, Weigel D. (1998) Gibberellins promote
893 flowering of arabidopsis by activating the LEAFY promoter. Plant Cell. 10(5):791-800.
894 Cao FY, Yoshioka K, Desveaux D. (2011) The roles of ABA in plant-pathogen interactions. J
895 Plant Res. 124(4):489-499.
896 Cao S, Ye M, Jiang S. (2005) Involvement of GIGANTEA gene in the regulation of the cold
897 stress response in Arabidopsis. Plant Cell Rep. 24(11):683-690.
898 Cao SQ, Song YQ, Su L. (2007) Freezing sensitivity in the *gigantea* mutant of *Arabidopsis* is
899 associated with sugar deficiency. Biol Plant. 51(2):359-362.
900 Carles C, Bies-Etheve N, Aspart L, Léon-Kloosterziel KM, Koornneef M, Echeverria M,
901 Delseny M. (2002) Regulation of Arabidopsis thaliana Em genes: role of ABI5. Plant J.
902 30(3):373-383.
903 Chang HC, Tsai MC, Wu SS, Chang IF. (2019) Regulation of ABI5 expression by ABF3
904 during salt stress responses in Arabidopsis thaliana. Bot Stud. 60(1):16.
905 Chen K, Li GJ, Bressan RA, Song CP, Zhu JK, Zhao Y. (2020) Abscisic acid dynamics,
906 signaling, and functions in plants. J Integr Plant Biol. 62(1):25-54.
907 Cheng MC, Liao PM, Kuo WW, Lin TP. (2013) The Arabidopsis ETHYLENE RESPONSE
908 FACTOR1 regulates abiotic stress-responsive gene expression by binding to different
909 cis-acting elements in response to different stress signals. Plant Physiol. 162(3):1566-
910 1582.
911 Choi H, Hong J, Ha J, Kang J, Kim SY. (2000) ABFs, a Family of ABA-responsive Element
912 Binding Factors. J Biol Chem. 275(3):1723-1730.
913 Conti L, Galbiati M, Tonelli C. (2014) ABA and the Floral Transition. In Abscisic Acid:
914 Metabolism, Transport and Signaling, D.-P. Zhang, ed (Springer Netherlands:
915 Dordrecht), pp. 365–384.
916 Covington MF, Harmer SL. (2007) The circadian clock regulates auxin signaling and
917 responses in Arabidopsis. PLoS Biol. 5(8):e222.
918 Covington MF, Maloof JN, Straume M, Kay SA, Harmer SL. (2008) Global transcriptome

analysis reveals circadian regulation of key pathways in plant growth and development. Genome Biol. 9(8): R130.

Cutler SR, Rodriguez PL, Finkelstein RR, Abrams SR. (2010) Abscisic acid: emergence of a core signaling network. Annu Rev Plant Biol. 61:651-679.

Dai A (2013) Increasing drought under global warming in observations and models. Nature Climate Change. 3:52–58.

Dalchau N, Baek SJ, Briggs HM, Robertson FC, Dodd AN, Gardner MJ, Stancombe MA, Haydon MJ, Stan GB, Gonçalves JM, Webb AA. (2011) The circadian oscillator gene GIGANTEA mediates a long-term response of the Arabidopsis thaliana circadian clock to sucrose. Proc Natl Acad Sci U S A. 108(102):5104-5109.

Dietz KJ, Sauter A, Wichert K, Messdaghi D, Hartung W. (2000) Extracellular beta-glucosidase activity in barley involved in the hydrolysis of ABA glucose conjugate in leaves. J Exp Bot. 51(346):937-944.

Domagalska MA, Sarnowska E, Nagy F, Davis SJ. (2010) Genetic analyses of interactions among gibberellin, abscisic acid, and brassinosteroids in the control of flowering time in Arabidopsis thaliana. PLoS One. 5(11):e14012.

Dong T, Park Y, Hwang I. (2015) Abscisic acid: biosynthesis, inactivation, homoeostasis and signalling. Essays Biochem. 58:29-48.

Edwards J, Martin AP, Andriunas F, Offler CE, Patrick JW, McCurdy DW. (2010) GIGANTEA is a component of a regulatory pathway determining wall ingrowth deposition in phloem parenchyma transfer cells of Arabidopsis thaliana. Plant J. 63(4):651-661.

Endo A, Sawada Y, Takahashi H, Okamoto M, Ikegami K, Koiwai H, Seo M, Toyomasu T, Mitsuhashi W, Shinozaki K, Nakazono M, Kamiya Y, Koshiba T, Nambara E. (2008) Drought induction of Arabidopsis 9-cis-epoxycarotenoid dioxygenase occurs in vascular parenchyma cells. Plant Physiol. 147(4):1984-1993.

Finkelstein R. (2013) Abscisic Acid Synthesis and Response. Arabidopsis Book. 11: e0166.

Finkelstein RR, Gampala SS, Rock CD. (2002) Abscisic acid signaling in seeds and seedlings. Plant Cell. S15-45.

Finkelstein RR, Lynch TJ. (2000) The Arabidopsis abscisic acid response gene ABI5 encodes a basic leucine zipper transcription factor. Plant Cell. 12(4):599-609.

Fornara F, Panigrahi KC, Gissot L, Sauerbrunn N, Rühl M, Jarillo JA, Coupland G. (2009)

951 Arabidopsis DOF transcription factors act redundantly to reduce CONSTANS
952 expression and are essential for a photoperiodic flowering response. Dev Cell.
953 17(1):75-86.
954 Fowler S, Lee K, Onouchi H, Samach A, Richardson K, Morris B, Coupland G, Putterill J.
955 (1999) GIGANTEA: a circadian clock-controlled gene that regulates photoperiodic
956 flowering in *Arabidopsis* and encodes a protein with several possible membrane-
957 spanning domains. EMBO J. 18(17):4679-4688.
958 Franks SJ, Sim S, Weis AE. (2007) Rapid evolution of flowering time by an annual plant in
959 response to a climate fluctuation. Proc Natl Acad Sci U S A. 104(4):1278-1282.
960 Frey A, Effroy D, Lefebvre V, Seo M, Perreau F, Berger A, Sechet J, To A, North HM,
961 Marion-Poll A. (2012) Epoxycarotenoid cleavage by NCED5 fine-tunes ABA
962 accumulation and affects seed dormancy and drought tolerance with other NCED
963 family members. Plant J. 70(3):501-512.
964 Fujita Y, Fujita M, Satoh R, Maruyama K, Parvez MM, Seki M, Hiratsu K, Ohme-Takagi M,
965 Shinozaki K, Yamaguchi-Shinozaki K. (2005) AREB1 is a transcription activator of
966 novel ABRE-dependent ABA signaling that enhances drought stress tolerance in
967 Arabidopsis. Plant Cell. 17(12):3470-3488.
968 Fukushima A, Kusano M, Nakamichi N, Kobayashi M, Hayashi N, Sakakibara H, Mizuno T,
969 Saito K. (2009) Impact of clock-associated Arabidopsis pseudo-response regulators in
970 metabolic coordination. Proc Natl Acad Sci U S A. 106(17):7251-7256.
971 Gehl C, Waadt R, Kudla J, Mendel RR, Hänsch R. (2009) New GATEWAY vectors for high
972 throughput analyses of protein-protein interactions by bimolecular fluorescence
973 complementation. Mol Plant. 2(5):1051-1058.
974 Gilbert ME, Medina V. (2016) Drought Adaptation Mechanisms Should Guide Experimental
975 Design. Trends Plant Sci. 21(8):639-647.
976 Grundy J, Stoker C, Carré IA. (2015) Circadian regulation of abiotic stress tolerance in plants.
977 Front Plant Sci. 6:648.
978 Han Y, Zhang X, Wang W, Wang Y, Ming F. (2013) The suppression of WRKY44 by
979 GIGANTEA-miR172 pathway is involved in drought response of Arabidopsis thaliana.
980 PLoS One. 8(11):e73541.
981 Han YJ, Cho KC, Hwang OJ, Choi YS, Shin AY, Hwang I, Kim JI (2012) Overexpression of
982 an Arabidopsis β-glucosidase gene enhances drought resistance with dwarf phenotype

983 in creeping bentgrass. Plant Cell Rep. 31(9):1677-1686.
984 Hao GP, Zhang XH, Wang YQ, Wu ZY, Huang CL. (2009) Nucleotide variation in the
985 NCED3 region of Arabidopsis thaliana and its association study with abscisic acid
986 content under drought stress. J Integr Plant Biol. 51(2):175-183.
987 Hauser F, Waadt R, Schroeder JI. (2011) Evolution of abscisic acid synthesis and signaling
988 mechanisms. Curr Biol. 21(9):R346-355.
989 Hirayama T, Shinozaki K (2007) Perception and transduction of abscisic acid signals: keys to
990 the function of the versatile plant hormone ABA. Trends Plant Sci. 12(8):343–351.
991 Huang D, Wu W, Abrams SR, Cutler AJ. (2008) The relationship of drought-related gene
992 expression in Arabidopsis thaliana to hormonal and environmental factors. J Exp Bot.
993 59(11):2991-3007.
994 Huang W, Pérez-García P, Pokhilko A, Millar AJ, Antoshechkin I, Riechmann JL, Mas P.
995 (2012) Mapping the core of the Arabidopsis circadian clock defines the network
996 structure of the oscillator. Science. 336(6077):75-79.
997 Imaizumi T, Schultz TF, Harmon FG, Ho LA, Kay SA. (2005) FKF1 F-Box Protein Mediates
998 Cyclic Degradation of a Repressor of CONSTANS in Arabidopsis. Science.
999 309(5732):293-297.
1000 Iuchi S, Kobayashi M, Taji T, Naramoto M, Seki M, Kato T, Tabata S, Kakubari Y,
1001 Yamaguchi-Shinozaki K, Shinozaki K. (2001) Regulation of drought tolerance by gene
1002 manipulation of 9-cis-epoxycarotenoid dioxygenase, a key enzyme in abscisic acid
1003 biosynthesis in Arabidopsis. Plant J. 27(4):325–333.
1004 Jensen MK, Lindemose S, de Masi F, Reimer JJ, Nielsen M, Perera V, Workman CT, Turck
1005 F, Grant MR, Mundy J, Petersen M, Skriver K. (2013) ATAF1 transcription factor
1006 directly regulates abscisic acid biosynthetic gene NCED3 in Arabidopsis thaliana.
1007 FEBS Open Bio. 3:321-327.
1008 Ji H, Pardo JM, Batelli G, Van Oosten MJ, Bressan RA, Li X. (2013) The Salt Overly
1009 Sensitive (SOS) pathway: established and emerging roles. Mol Plant. 6(2):275-286.
1010 Jiang Y, Liang G, Yu D. (2012) Activated expression of WRKY57 confers drought tolerance
1011 in Arabidopsis. Mol Plant. 5(6):1375-1388.
1012 Kazan K. (2015) Diverse roles of jasmonates and ethylene in abiotic stress tolerance. Trends
1013 Plant Sci. 20(4):219-229.
1014 Kidokoro S, Maruyama K, Nakashima K, Imura Y, Narusaka Y, Shinwari ZK, Osakabe Y,

Fujita Y, Mizoi J, Shinozaki K, Yamaguchi-Shinozaki K. (2009) The phytochrome-interacting factor PIF7 negatively regulates DREB1 expression under circadian control in Arabidopsis. Plant Physiol. 151(4):2046-57.

Kim H, Kim SH, Seo DH, Chung S, Kim SW, Lee JS, Kim WT, Lee JH. (2016) ABA-HYPERSENSITIVE BTB/POZ PROTEIN 1 functions as a negative regulator in ABA-mediated inhibition of germination in Arabidopsis. Plant Mol Biol. 90(3):303-315.

Kim JH, Hyun WY, Nguyen HN, Jeong CY, Xiong L, Hong SW, Lee H. (2015) AtMyb7, a subgroup 4 R2R3 Myb, negatively regulates ABA-induced inhibition of seed germination by blocking the expression of the bZIP transcription factor ABI5. Plant Cell Environ. 38(3):559-571.

Kim SY (2006) The role of ABF family bZIP class transcription factors in stress response. Physiol. Plant. 126:519-527.

Kim WY, Ali Z, Park HJ, Park SJ, Cha JY, Perez-Hormaeche J, Quintero FJ, Shin G, Kim MR, Qiang Z, Ning L, Park HC, Lee SY, Bressan RA, Pardo JM, Bohnert HJ, Yun DJ. (2013) Release of SOS2 kinase from sequestration with GIGANTEA determines salt tolerance in Arabidopsis. Nat Commun. 4:1352.

Kim WY, Fujiwara S, Suh SS, Kim J, Kim Y, Han L, David K, Putterill J, Nam HG, Somers DE. (2007) ZEITLUPE is a circadian photoreceptor stabilized by GIGANTEA in blue light. Nature. 449(7160):356-360.

Koornneef M, Hanhart CJ, van der Veen JH. (1991) A genetic and physiological analysis of late flowering mutants in *Arabidopsis thaliana*. Mol Gen Genet. 229(1):57-66.

Kubota A, Ito S, Shim JS, Johnson RS, Song YH, Breton G, Goralogia GS, Kwon MS, Laboy Cintrón D, Koyama T, Ohme-Takagi M, Pruneda-Paz JL, Kay SA, MacCoss MJ, Imaizumi T. (2017) TCP4-dependent induction of CONSTANS transcription requires GIGANTEA in photoperiodic flowering in Arabidopsis. PLoS Genet. 13(6):e1006856.

Kudo M, Kidokoro S, Yoshida T, Mizoi J, Todaka D, Fernie AR, Shinozaki K, Yamaguchi-Shinozaki K. (2017) Double overexpression of DREB and PIF transcription factors improves drought stress tolerance and cell elongation in transgenic plants. Plant Biotechnol J. 15(4):458-471.

Kurepa J, Smalle J, Van Montagu M, Inzé D. (1998) Oxidative stress tolerance and longevity in Arabidopsis: the late-flowering mutant gigantea is tolerant to paraquat. Plant J. 14(6):759-764.

1047 Kurup S, Jones HD, Holdsworth MJ. (2000) Interactions of the developmental regulator
1048 ABI3 with proteins identified from developing Arabidopsis seeds. Plant J. 21(2):143-
1049 155.
1050 Kushiro T, Okamoto M, Nakabayashi K, Yamagishi K, Kitamura S, Asami T, Hirai N,
1051 Koshiba T, Kamiya Y, Nambara E (2004) The Arabidopsis cytochrome P450 CYP707A
1052 encodes ABA 8′-hydroxylases: key enzymes in ABA catabolism. EMBO J. 23(7):1647–
1053 1656.
1054 Lee HG, Lee K, Seo PJ. (2015) The Arabidopsis MYB96 transcription factor plays a role in
1055 seed dormancy. Plant Mol Biol. 87(4-5):371-381.
1056 Lee HG, Mas P, Seo PJ. (2016) MYB96 shapes the circadian gating of ABA signaling in
1057 Arabidopsis. Sci Rep. 6:17754.
1058 Lee KH, Piao HL, Kim HY, Choi SM, Jiang F, Hartung W, Hwang I, Kwak JM, Lee IJ,
1059 Hwang I. (2006) Activation of glucosidase via stress-induced polymerization rapidly
1060 increases active pools of abscisic acid. Cell. 126(6):1109-1120.
1061 Lefebvre V, North H, Frey A, Sotta B, Seo M, Okamoto M, Nambara E, Marion Poll A. (2006)
1062 Functional analysis of Arabidopsis NCED6 and NCED9 genes indicates that ABA
1063 synthesized in the endosperm is involved in the induction of seed dormancy. Plant J.
1064 45(3):309–319.
1065 Legnaioli T, Cuevas J, Mas P. (2009) TOC1 functions as a molecular switch connecting the
1066 circadian clock with plant responses to drought. EMBO J. 28(23):3745-3757.
1067 Lim S, Park J, Lee N, Jeong J, Toh S, Watanabe A, Kim J, Kang H, Kim DH, Kawakami N,
1068 Choi G. (2013) ABA-insensitive3, ABA-insensitive5, and DELLAs Interact to activate
1069 the expression of SOMNUS and other high-temperature-inducible genes in imbibed
1070 seeds in Arabidopsis. Plant Cell. 25(12):4863-4878.
1071 Liu T, Carlsson J, Takeuchi T, Newton L, Farré EM. (2013) Direct regulation of abiotic
1072 responses by the Arabidopsis circadian clock component PRR7. Plant J. 76(1):101-114.
1073 Martínez-Andújar C, Ordiz MI, Huang Z, Nonogaki M, Beachy RN, Nonogaki H. (2011)
1074 Induction of 9-cis-epoxycarotenoid dioxygenase in Arabidopsis thaliana seeds enhances
1075 seed dormancy. Proc Natl Acad Sci USA. 108(21):17225–17229.
1076 Michael TP, Breton G, Hazen SP, Priest H, Mockler TC, Kay SA, Chory J. (2008) A morning-
1077 specific phytohormone gene expression program underlying rhythmic plant growth.
1078 PLoS Biol. 6(9):e225.

Mishra P, Panigrahi KC. (2015) GIGANTEA - an emerging story. Front Plant Sci. 6:8.

Mizoguchi T, Wright L, Fujiwara S, Cremer F, Lee K, Onouchi H, Mouradov A, Fowler S, Kamada H, Putterill J, Coupland G. (2005) Distinct roles of GIGANTEA in promoting flowering and regulating circadian rhythms in *Arabidopsis.* Plant Cell. 17(8):2255-2270.

Mizuno T, Yamashino T. (2008) Comparative transcriptome of diurnally oscillating genes and hormone-responsive genes in Arabidopsis thaliana: insight into circadian clock-controlled daily responses to common ambient stresses in plants. Plant Cell Physiol. 49(3):481-487.

Nakagawa T, Kurose T, Hino T, Tanaka K, Kawamukai M, Niwa Y, Toyooka K, Matsuoka K, Jinbo T, Kimura T. (2007) Development of series of gateway binary vectors, pGWBs, for realizing efficient construction of fusion genes for plant transformation. J Biosci Bioeng. 104(1):34-41.

Nakamichi N, Kiba T, Henriques R, Mizuno T, Chua NH, Sakakibara H. (2010) PSEUDO-RESPONSE REGULATORS 9, 7, and 5 are transcriptional repressors in the Arabidopsis circadian clock. Plant Cell. 22(3):594-605.

Nakamichi N, Kiba T, Kamioka M, Suzuki T, Yamashino T, Higashiyama T, Sakakibara H, Mizuno T. (2012) Transcriptional repressor PRR5 directly regulates clock-output pathways. Proc Natl Acad Sci U S A. 109(42):17123-17128.

Nambara E, Marion-Poll A. (2005) Abscisic acid biosynthesis and catabolism. Annu Rev Plant Biol. 56:165-185.

Nováková M, Motyka V, Dobrev PI, Malbeck J, Gaudinová A, Vanková R. (2005) Diurnal variation of cytokinin, auxin and abscisic acid levels in tobacco leaves. J Exp Bot. 56(421):2877-2883.

Okamoto M, Kuwahara A, Seo M, Kushiro T, Asami T, Hirai N, Kamiya Y, Koshiba T, Nambara E (2006) CYP707A1 and CYP707A2, which encode abscisic acid 8′-hydroxylases, are indispensable for proper control of seed dormancy and germination in Arabidopsis. Plant Physiol 141(1):97–107.

Park DH, Somers DE, Kim YS, Choy YH, Lim HK, Soh MS, Kim HJ, Kay SA, Nam HG. (1999) Control of circadian rhythms and photoperiodic flowering by the *Arabidopsis* GIGANTEA gene. Science. 285(5433):1579-1582.

Park J, Lim CJ, Khan IU, Jan M, Khan HA, Park HJ, Guo Y, Yun DJ. (2018) Identification and Molecular Characterization of HOS15-interacting Proteins in Arabidopsis thaliana.

J. Plant Biol. 61:336-345

Penfield S, Hall A. (2009) A role for multiple circadian clock genes in the response to signals that break seed dormancy in Arabidopsis. Plant Cell. 21(6):1722-1732.

Qin X, Zeevaart JA. (2002) Overexpression of a 9-cis-epoxycarotenoid dioxygenase gene in Nicotiana plumbaginifolia increases abscisic acid and phaseic acid levels and enhances drought tolerance. Plant Physiol. 128(2):544–551.

Quintero FJ, Martinez-Atienza J, Villalta I, Jiang X, Kim WY, Ali Z, Fujii H, Mendoza I, Yun DJ, Zhu JK, Pardo JM. (2011) Activation of the plasma membrane Na/H antiporter Salt-Overly-Sensitive 1 (SOS1) by phosphorylation of an auto-inhibitory C-terminal domain. Proc Natl Acad Sci U S A. 108(6):2611-2616.

Riboni M, Galbiati M, Tonelli C, Conti L. (2013) GIGANTEA enables drought escape response via abscisic acid-dependent activation of the florigens and SUPPRESSOR OF OVEREXPRESSION OF CONSTANS. Plant Physiol. 162(3):1706-1719.

Riboni M, Robustelli Test A, Galbiati M, Tonelli C, Conti L. (2016) ABA-dependent control of GIGANTEA signalling enables drought escape via up-regulation of FLOWERING LOCUS T in Arabidopsis thaliana. J Exp Bot. 67(22):6309-6322.

Saito S, Hirai N, Matsumoto C, Ohigashi H, Ohta D, Sakata K, Mizutani M (2004) Arabidopsis CYP707As encode (+)-abscisic acid 8′-hydroxylase, a key enzyme in the oxidative catabolism of abscisic acid. Plant Physiol. 134(4):1439–1449.

Sakuraba Y, Han SH, Lee SH, Hörtensteiner S, Paek NC. (2016) Arabidopsis NAC016 promotes chlorophyll breakdown by directly upregulating STAYGREEN1 transcription. Plant Cell Rep. 35(1):155-166.

Saleh A, Alvarez-Venegas R, Avramova Z. (2008) An efficient chromatin immunoprecipitation (ChIP) protocol for studying histone modifications in Arabidopsis plants. Nat Protoc. 3(6):1018-1025.

Salomé PA, Xie Q, McClung CR. (2008) Circadian timekeeping during early Arabidopsis development. Plant Physiol. 147(3):1110-1125.

Sato H, Takasaki H, Takahashi F, Suzuki T, Iuchi S, Mitsuda N, Ohme-Takagi M, Ikeda M, Seo M, Yamaguchi-Shinozaki K, Shinozaki K. (2018) Arabidopsis thaliana NGATHA1 transcription factor induces ABA biosynthesis by activating NCED3 gene during dehydration stress. Proc Natl Acad Sci U S A. 115(47):E11178-E11187.

Sawa M, Nusinow DA, Kay SA, Imaizumi T. (2007) FKF1 and GIGANTEA Complex

1143 Formation Is Required for Day-Length Measurement in Arabidopsis. Science.
1144 318(5848):261-265.
1145 Schwartz SH, Tan BC, McCarty DR, Welch W, Zeevaart JA. (2003) Substrate specificity and
1146 kinetics for VP14, a carotenoid cleavage dioxygenase in the ABA biosynthetic pathway.
1147 Biochim Biophys Acta. 1619(1):9-14.
1148 Seo M, Hanada A, Kuwahara A, Endo A, Okamoto M, Yamauchi Y, North H, Marion-Poll A,
1149 Sun TP, Koshiba T, Kamiya Y, Yamaguchi S, Nambara E. (2006) Regulation of
1150 hormone metabolism in Arabidopsis seeds: phytochrome regulation of abscisic acid
1151 metabolism and abscisic acid regulation of gibberellin metabolism. Plant J. 48(3):354-
1152 366.
1153 Seo M, Koshiba T. (2002) Complex regulation of ABA biosynthesis in plants. Trends Plant
1154 Sci. 7(1):41–48.
1155 Seung D, Risopatron JP, Jones BJ, Marc J. (2012) Circadian clock-dependent gating in ABA
1156 signalling networks. Protoplasma. 249(3):445-457.
1157 Singh M, Mas P. (2018) A functional connection between the circadian clock and hormonal
1158 timing in Arabidopsis. Genes (Basel) 9:567.
1159 Sirichandra C, Wasilewska A, Vlad F, Valon C, Leung J. (2009) The guard cell as a single-
1160 cell model towards understanding drought tolerance and abscisic acid action. J Exp Bot.
1161 60(5):1439-1463.
1162 Skubacz A, Daszkowska-Golec A, Szarejko I. (2016) The Role and Regulation of ABI5
1163 (ABA-Insensitive 5) in Plant Development, Abiotic Stress Responses and
1164 Phytohormone Crosstalk. Front Plant Sci. 7:1884.
1165 Song JB, Gao S, Sun D, Li H, Shu XX, Yang ZM. (2013) miR394 and LCR are involved in
1166 Arabidopsis salt and drought stress responses in an abscisic acid-dependent manner.
1167 BMC Plant Biol. 13:210.
1168 Suarez-Lopez P, Wheatley K, Robson F, Onouchi H, Valverde F, Coupland G (2001)
1169 CONSTANS mediates between the circadian clock and the control of flowering in
1170 Arabidopsis. Nature. 410(6832):1116-1120.
1171 Swarup K, Alonso-Blanco C, Lynn JR, Michaels SD, Amasino RM, Koornneef M, Millar AJ.
1172 (1999) Natural allelic variation identifies new genes in the Arabidopsis circadian
1173 system. Plant J. 20(1):67-77.
1174 Tan BC, Joseph LM, Deng WT, Liu L, Li QB, Cline K, McCarty DR. (2003) Molecular

characterization of the Arabidopsis 9-cis epoxycarotenoid dioxygenase gene family. Plant J. 35(1):44-56.

Tan W, Zhang D, Zhou H, Zheng T, Yin Y, Lin H. (2018) Transcription factor HAT1 is a substrate of SnRK2.3 kinase and negatively regulates ABA synthesis and signaling in Arabidopsis responding to drought. PLoS Genet. 14(4):e1007336.

Thain SC, Vandenbussche F, Laarhoven LJ, Dowson-Day MJ, Wang ZY, Tobin EM, Harren FJ, Millar AJ, Van Der Straeten D. (2004) Circadian rhythms of ethylene emission in Arabidopsis. Plant Physiol. 136(3):3751-3761.

Thompson AJ, Jackson AC, Parker RA, Morpeth DR, Burbidge A, Taylor IB. (2000) Abscisic acid biosynthesis in tomato: regulation of zeaxanthin epoxidase and 9-cis-epoxycarotenoid dioxygenase mRNAs by light/dark cycles, water stress and abscisic acid. Plant Mol Biol. 42(6):833-845.

Tian G, Lu Q, Zhang L, Kohalmi SE, Cui Y. (2011) Detection of protein interactions in plant using a gateway compatible bimolecular fluorescence complementation (BiFC) system. J Vis Exp. (55). e3473.

Tseng TS, Salomé PA, McClung CR, Olszewski NE. (2004) SPINDLY and GIGANTEA interact and act in Arabidopsis thaliana pathways involved in light responses, flowering, and rhythms in cotyledon movements. Plant Cell. 16(6):1550-1563.

Wasternack C, Hause B. (2013) Jasmonates: biosynthesis, perception, signal transduction and action in plant stress response, growth and development. An update to the 2007 review in Annals of Botany. Ann Bot. 111(6):1021-1058.

Xiong L, Schumaker KS, Zhu JK. (2002) Cell signaling during cold, drought, and salt stress. Plant Cell. 14. Suppl:S165-183.

Xu ZJ, Nakajima M, Suzuki Y, Yamaguchi I. (2002) Cloning and characterization of the abscisic acid-specific glucosyltransferase gene from adzuki bean seedlings. Plant Physiol. 129(3):1285-1295.

Yang O, Popova OV, Süthoff U, Lüking I, Dietz KJ, Golldack D. (2009) The Arabidopsis basic leucine zipper transcription factor AtbZIP24 regulates complex transcriptional networks involved in abiotic stress resistance. Gene. 436(1-2):45-55.

Yang WT, Baek D, Yun DJ, Lee KS, Hong SY, Bae KD, Chung YS, Kwon YS, Kim DH, Jung KH, Kim DH. (2018) Rice OsMYB5P improves plant phosphate acquisition by regulation of phosphate transporter. PLoS One. 13(3):e0194628.

Yang Y, Qi M, Mei C. (2004) Endogenous salicylic acid protects rice plants from oxidative damage caused by aging as well as biotic and abiotic stress. Plant J. 40(6):909-919.

Yu JW, Rubio V, Lee NY, Bai S, Lee SY, Kim SS, Liu L, Zhang Y, Irigoyen ML, Sullivan JA, Zhang Y, Lee I, Xie Q, Paek NC, Deng XW. (2008) COP1 and ELF3 control circadian function and photoperiodic flowering by regulating GI stability. Mol. Cell 32(5):617-630.

Zhu JK. (2016) Abiotic Stress Signaling and Responses in Plants. Cell. 167(2):313-324.

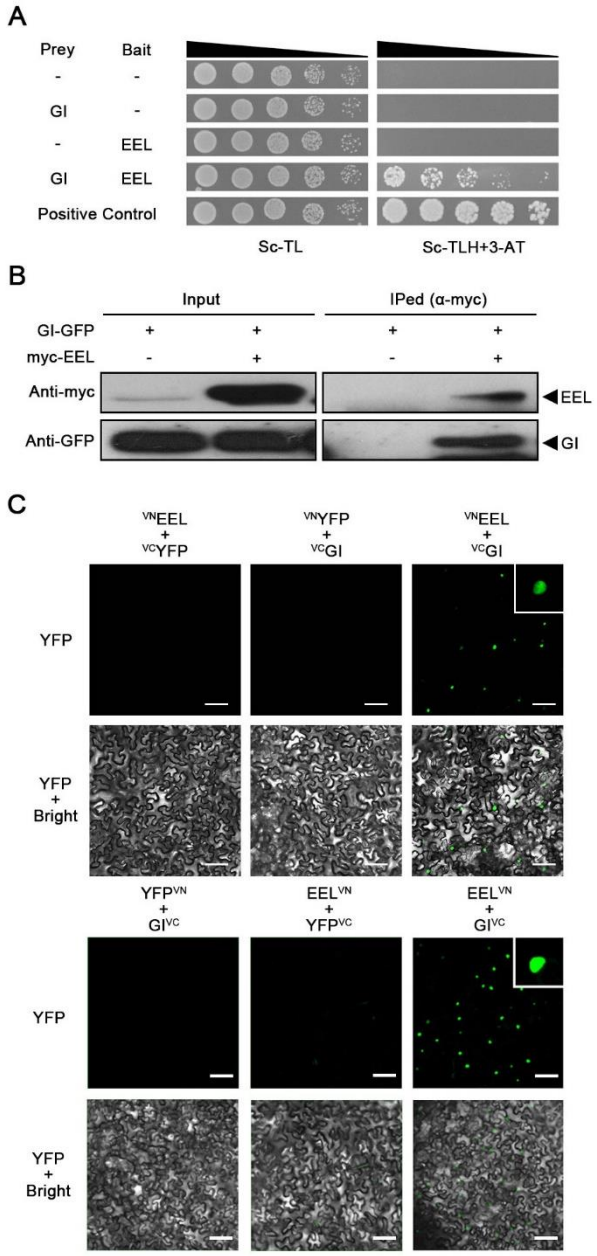

Figure 1. Interaction between the GI and EEL proteins.

(A) Protein-protein interaction assay using a yeast two-hybrid system. Prey is the *pDEST22* plasmid with the AD domain of GAL4, and Bait is the *pDEST32* plasmid with BD domain. Yeast cells co-transformed with GI-AD and EEL-BD were plated on the control SC-TL and selective medium SC-TLH with 25 mM 3-AT. The combinations with empty vector plasmids were used as negative controls. (B) Co-immunprecipitation assay with EEL and GI proteins. Total proteins extracted from *Nicotiana benthamiana* leaves co-infiltrated with GI-GFP and myc-EEL constructs. Input levels of epitope tagged proteins in total protein extracts were analyzed by immunoblotting with anti-myc and anti-GFP antibodies. Immunoprecipitated

myc-tagged proteins were probed with anti-GFP antibody to detect co-immunoprecipitation of GI-GFP with myc-EEL. (C) GI and EEL interaction using BiFC assays in tobacco cells. The VN and VC represent the N- and C- terminal domain of Venus (eYFP), respectively. The GI-EEL complex was localized to the nucleus of the tobacco leaf epidermal cells. Plasmid combinations of ^{VN}EEL and ^{VC}GI (Upper) or EEL^{VN} and GI^{VC} (Bottom) are indicated above the images. The combinations with empty vector plasmids were used as negative controls. Scale bars represented 100 μm.

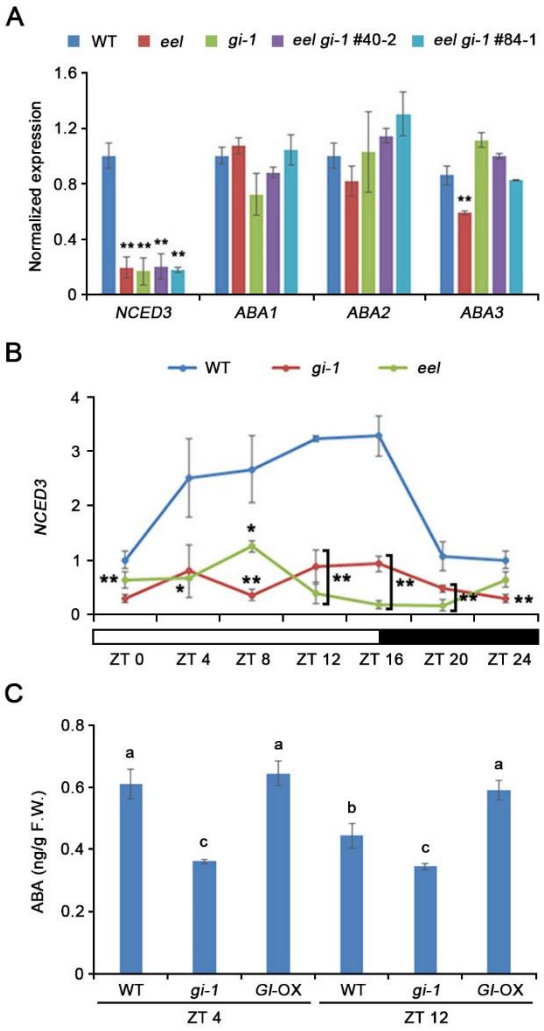

Figure 2. The diurnal expression of the ABA biosynthesis-related gene *NCED3* requires EEL and GI.

(A) Transcript levels of *NCED3*, *ABA1*, *ABA2*, and *ABA3* in WT plants, *eel*, *gi-1*, and *eel gi-1* mutants. The 10-day-old seedlings grown on 1/2 MS medium under long-day cycles were sampled 4 hours after dawn (ZT4) and submitted to total RNA extraction. The transcript levels of *NCED3*, *ABA1*, *ABA2* and *ABA3* were measured using qRT-PCR. The *TUBULIN2* was used as an internal control for normalization. Error bars represent the SD from three biological replicates, each with three technical replicates. Asterisks represent significant differences from the WT (**, p-value ≤ 0.01, Student's t-test). (B) Transcript levels of *NCED3* were analyzed in WT plants and *gi-1* or *eel* mutants grown on 1/2 MS medium for 10 days under a long-day photoperiod. Transcript levels were measured using qRT-PCR from total RNA extracted from seedlings at different ZT times. The white and black bars below the plot indicate the light and darkness periods, respectively. *TUBULIN2* was used as an internal control for normalization.

Error bars represent the SD from three biological replicates, each with three technical replicates. Asterisks represent significant differences from WT (*, 0.01 < *p*-value ≤ 0.05, **, *p*-value ≤ 0.01, Student's *t*-test). (C) ABA content in 10-day-old seedlings of wild-type (WT), *gi-1* and *GI*-OX plants grown on 1/2 MS medium under long-day cycles and sampled 4 and 12 hours after dawn (ZT4 and ZT12). ABA contents were measured from 20 whole seedlings of each genotype. Error bars represent the SD from three biological replicates, each with three technical replicates. Different letters indicate significantly different values at p-value ≤ 0.05 determined by one-way ANOVA.

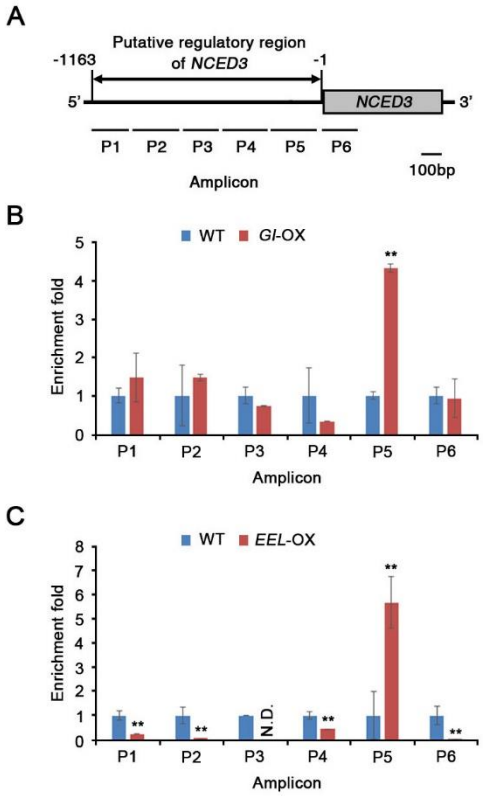

Figure 3. EEL and GI associate with the *NCED3* promoter *in vivo*.

(A) Schematic drawing of the *NCED3* locus and locations of the ChIP assay amplicons (P1 to P6). The 1,000 bp upstream of the transcription start site on the *NCED3* genes was used. (B, C) The ChIP assay of the *NCED3* chromatin regions associated with GI and EEL. The ChIP assays were performed on nuclear proteins extracted from 10-day-old seedling of wild-type (WT) and those of *GI*-OX (B) or *EEL*-OX (C) seedlings. Plants were grown on 1/2 x MS under long-day conditions. Samples were prepared for the ChIP analysis using an anti-HA (B) or anti-myc antibody (C). The immunoprecipitated DNA was amplified using qRT-PCR with specific primers for the amplicons. The *TUBULIN2* was used as an internal control for normalization. The fold enrichment is the ratio of *GI*-OX or *EEL*-OX to WT signal. N.D. means not detected. Error bars represent the SD from three biological replicates, each with three technical replicates. Asterisks represent significant differences from the WT (**, p-value ≤ 0.01, Student's t-test).

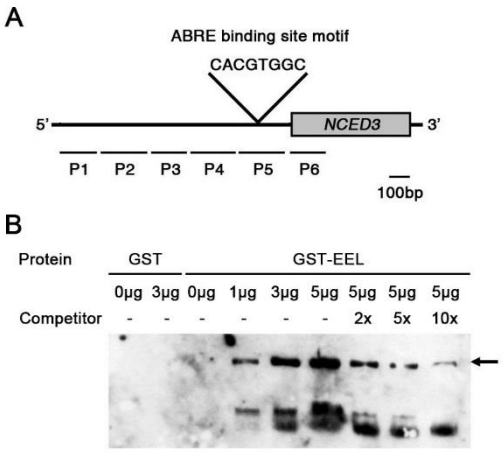

Figure 4. EEL bind to the *NCED3* promoter.

(A) Schematic drawing of the ABRE binding site motif locus and sequence in the *NCED3* promoter. (B) The EMSAs were conducted using the GST-EEL fusion protein. The probe containing the ABRE binding site motif was biotin-labeled for use in the reaction. Unlabeled probes were also included in the reaction as competitors in the specified ratios to the biotin-labeled probe. The arrow indicates the EEL protein and ABRE probe complex.

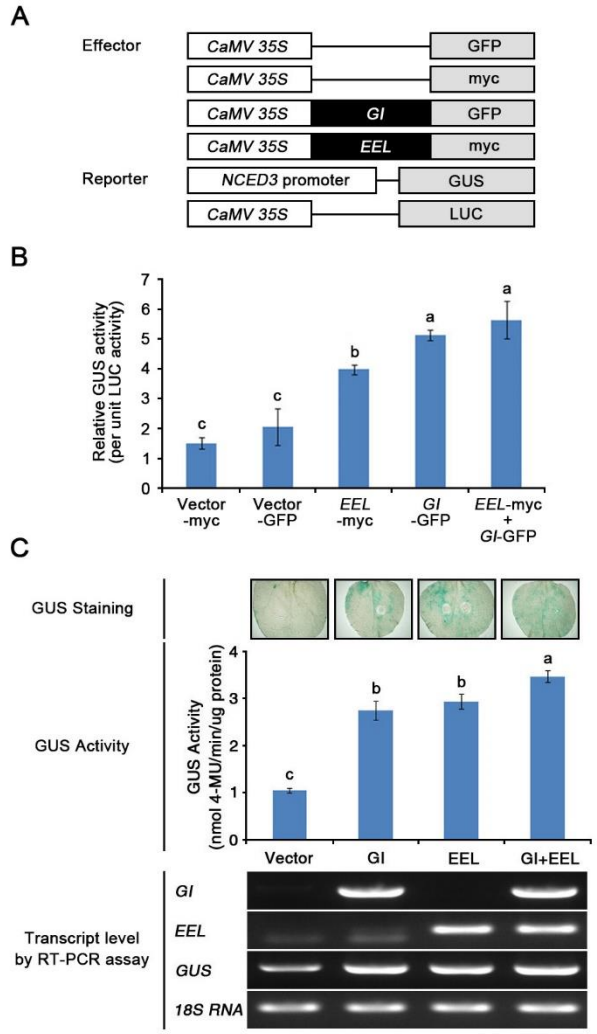

Figure 5. Transcriptional activity assay of GI and EEL.

(A) A schematic representation of the effector and reporter constructs used in the transient expression assay. (B) Protoplasts were isolated from the leaves of 3-week-old *Arabidopsis* plants, and were co-transfected with the reporter plasmids NCED3:GUS and 35S:LUC, and with one of the effector plasmids (empy vector-GFP, GI-GFP, empty vector-myc, and EEL-myc). The *35S:LUC* plasmid was used for signal normalization. The GUS reporter activity in each sample combination is presented as the GUS/LUC ratio. (C) The *NCED3* promoter was fused to *GUS* and co-expressed in tobacco leaves together with different combinations of EEL and GI. The images of GUS staining in the top panels show leaves expressing the indicated constructs. The middle panel presents the quantification of GUS activity. The bottom panel shows transcript levels of *GI*, *EEL*, or *GUS* in infiltrated tobacco leaves quantified using RT-PCR. Tobacco *18S rRNA* expression was detected as a loading control. Error bars represent the SD from three independent experiments. Different letters indicate significantly different values

at p-value $\leq$ 0.05 determined by one-way ANOVA.

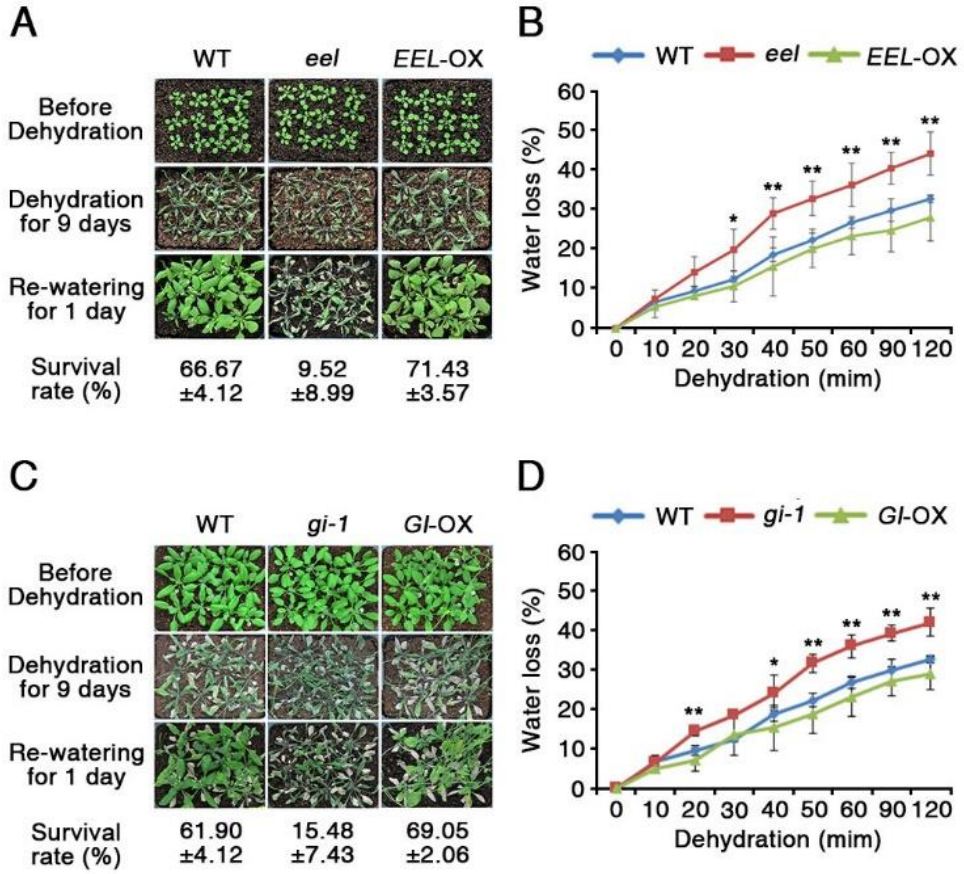

Figure 6. Characterization of the drought responses of the *eel* and *gi-1* mutants.

Drought stress response of wild-type (WT), *eel,* and *EEL*-OX (A, B) or *gi-1* and *GI*-OX (C, D) plants. The plants were grown in soil with sufficient water for two weeks (upper panel in A and C), then water was withheld for 9 days (middle panels in A and C). The drought stress was then alleviated by re-watering the plants for one day (bottom panels in A and C). The survival rates of the plants were determined from three replicates, each of which involved at least 12 plants. (B, D) Water loss by transpiration was measured from detached leaves of four-week-old WT, *eel*, and *EEL*-OX (B) or *gi-1*, and *GI*-OX (D) plants. The water loss at each time point was calculated as a percentage of the initial fresh weight (n=10). Error bars represent the SD from three independent experiments. Asterisks represent significant differences from the WT (*, 0.01 < p-value ≤ 0.05; **, p-value ≤ 0.01, Student's t-test).

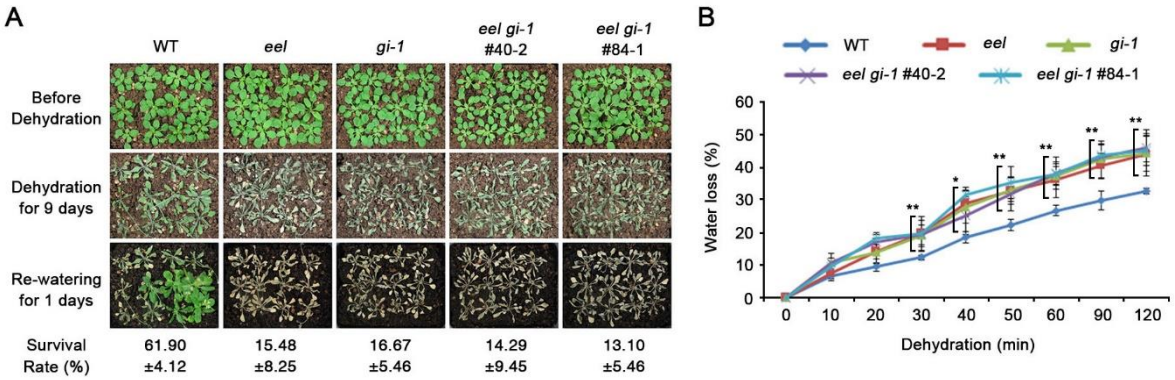

Figure 7. Characterization of the drought stress responses of the *eel gi-1* double mutants. (A) Wild-type (WT) plants, and *eel*, *gi-1*, and *eel gi-1* mutants were grown in soil with sufficient water for three weeks (upper panels), then water was withheld for nine days (middle panels). The drought-stressed plants were then re-watered for one day (bottom panel), after which their survival rates were assessed. Each experiment comprised at least 12 plants, and three replicates were performed. (B) Water loss by transpiration was measured from the leaves of WT plants, *eel*, *gi-1*, and *eel gi-1* mutants. The shoots of three-week-old plants were detached and their water loss at each time point was calculated as a percentage of their initial fresh weight (n=10). Error bars represent SD from three independent experiments. Asterisks represent significant differences from the WT (*, $0.01 < p$-value ≤ 0.05; **, p-value ≤ 0.01, Student's t-test).

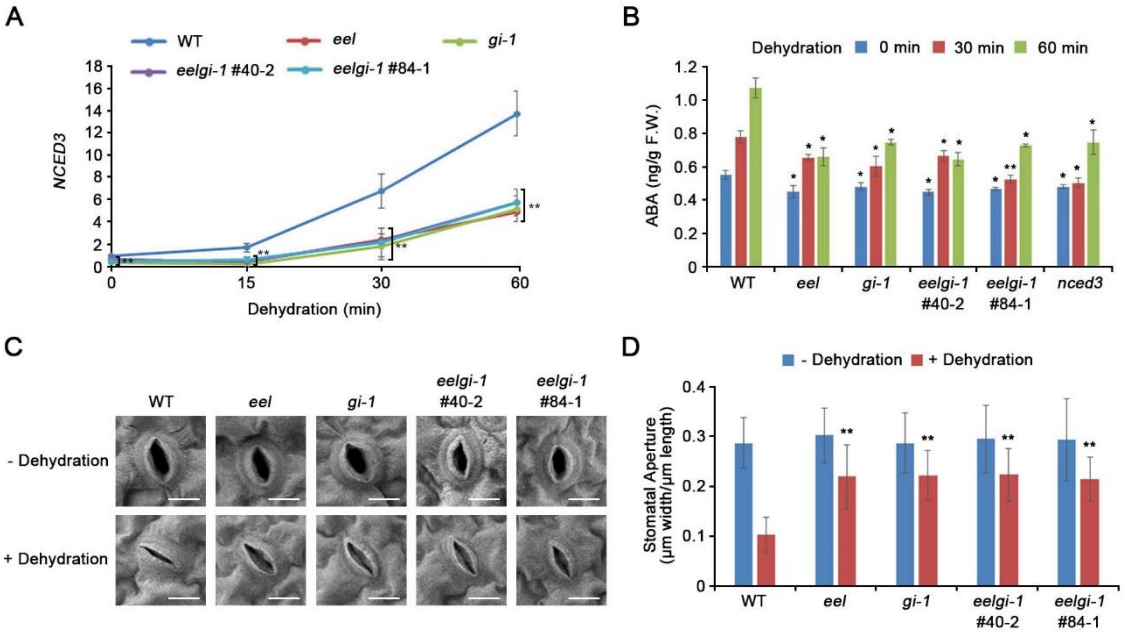

Figure 8. The expression of *NCED3*, ABA levels and stomatal closure in WT plants, the *eel*, *gi-1*, and *eel gi-1* mutants under drought stress condition.

(A) Transcript levels of *NCED3* in wild-type (WT) plants, and of *eel*, *gi-1*, and *eel gi-1* mutants over 1-hour dehydration stress. Ten-day-old seedlings grown on 1/2 MS medium under long-day cycles were sampled at ZT4 (control non-treated sample) and again 30 and 60 minutes after a dehydration treatment. *NCED3* transcript levels were measured using qRT-PCR. The expression of *TUBULIN2* was used as an internal control for normalization. Error bars represent the SD of three biological replicates, each with three technical replicates. (B) ABA content in seedlings treated as in (A). ABA contents were measured from 20 whole seedlings of each genotype. Error bars represent the SD from four independent experiments. (C) The rosette leaf epidermis of WT plants, *eel*, *gi-1* and *eel gi-1* mutants were floated in stomatal opening solution for 2 h, and then removed and placed onto filter paper for 1h for the dehydration treatment. Stomata on the abaxial surface were observed using scanning electron microscopy. Scale bar indicates 10 µm. (D) Measurement of stomatal apertures (width/length) in WT plants, *eel*, *gi-1* and *eel gi-1* mutants before and after dehydration for 1h. Error bars represent the SD from three independent experiments, with at least 30 stomata measured per genotype and per treatment. Asterisks represent significant differences from the WT (*, 0.01 < *p*-value ≤ 0.05; **, p-value ≤ 0.01, Student's *t*-test).

SUPPLEMENTARY FIGURES

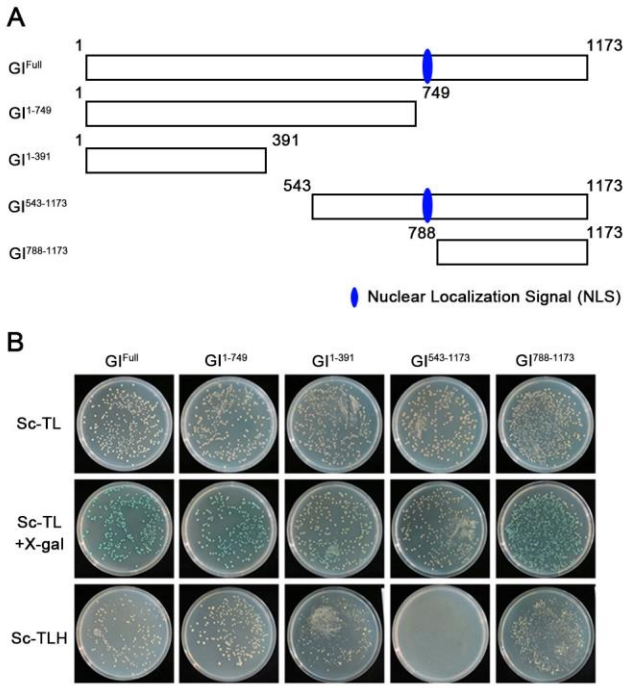

Supplementary Figure S1. Auto-activation between the GI protein and the GAL4 activation domain (AD) in the Matchmaker yeast two-hybrid screen system.

(A) Schematic representations of the full-length and truncated GI proteins used in the assay. (B) Auto-activation assay of the full-length and truncated GI proteins fused in-frame with the GAL4 DNA-binding domain (BD) of the pGBK7 bait vector. Co-transformed yeast colonies with auto-activity showed blue color in plates with 40 μg/mL X-gal and were able to grow on selective medium SC-TLH.

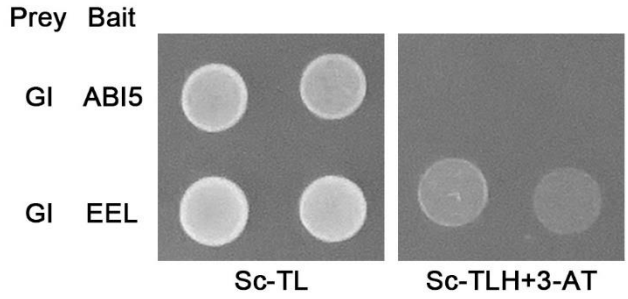

Supplementary Figure S2. Yeast-two-hybrid assay of GI and ABI5 proteins.
Yeast cells co-transformed with GI (Prey, pDEST22) and ABI5 (Bait, pDEST32) were plated on the control SC-TL and selective medium SC-TLH plus 25 mM 3-AT. The combinations with GI (Prey) and EEL (Bait) were used as positive control.

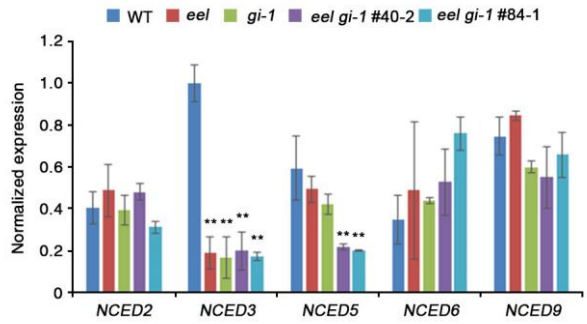

Supplementary Figure S3. The expression of *NCED* family genes in WT plants, *eel*, *gi-1*, and *eel gi-1* mutants.

Transcript levels of *NCED2*, *NCED3*, *NCED5*, *NCED6*, and *NCED9* were analyzed in plants grown on 1/2 MS medium for 10 days under a long-day photoperiod. Transcript levels were measured using qRT-PCR from total RNA extracted from seedlings at ZT4. *TUBULIN2* was used as an internal control for normalization. Error bars represent the SD from three biological replicates, each with three technical replicates. Asterisks represent significant differences from WT (**, p-value ≤ 0.01, Student's t-test).

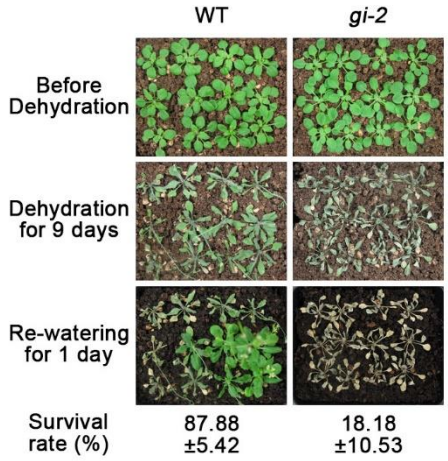

Supplementary Figure S4. Characterization of the drought stress response of the *gi-2* mutant. Wild-type (WT) and *gi-2* mutant plants were grown in soil with sufficient water for two weeks (upper panels), and then water was withheld for 9 days (middle panels). The drought stress was alleviated by re-watering the plants for one day (bottom panels). The survival rates of the plants were determined from three replicates, each of which involved at least 28 plants.

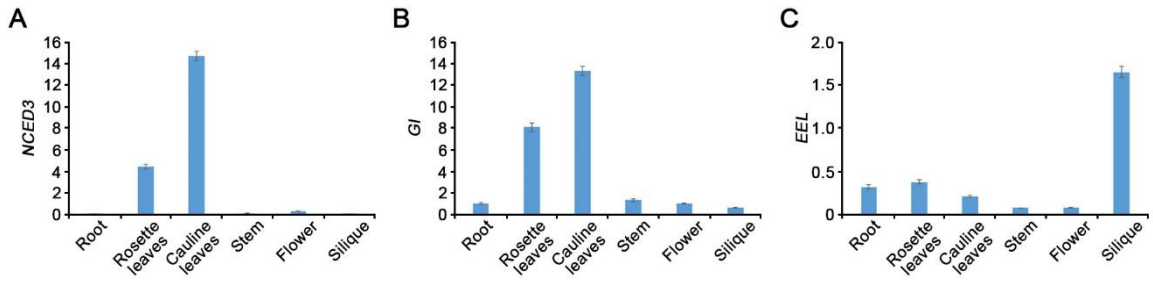

Supplementary Figure S5. The expression of *NCED3*, *GI* and *EEL* in various tissues of *Arabidopsis thaliana*.

Total RNA was extracted from the roots, rosette leaves, cauline leaves, stems, flowers, and siliques of wild-type plants. The transcript levels of *NCED3*, *GI* and *EEL* were measured using qRT-PCR. *TUBULIN2* was used as an internal control for normalization. Error bars represent the SD from three biological replicates, each with three technical replicates.

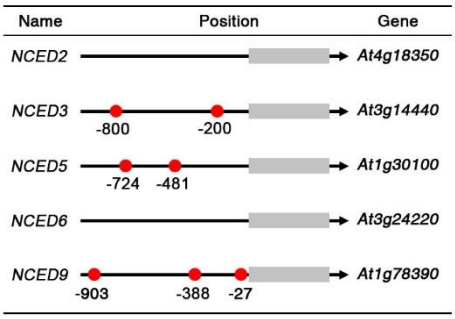

Supplementary Figure S6. Putative ABRE *cis*-acting regulatory elements in the promoters of the *NCED* family.

The 1,000 bp upsteam of the transcription start site on the NCED genes was analyzed. Red dots indicate the ABRE binding site motifs [(*C*/*T*)*ACGTGGC*; (*C*/*G*)*ACGTG*(*T*/*G*)(*C*/*A*); *TACGGTC*] (Heidari et al., 2015). The positions are labeled relative to the transcription start site using PlantCARE database (http://bioinformatics.psb.ugent.be/webtools/plantcare/html/).

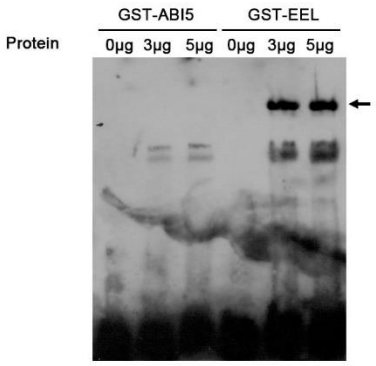

Supplementary Figure S7. EMSA using ABI5 and the ABRE binding site motif in the *NCED3* promoter.

The EMSA was conducted using the GST-ABI5 and GST-EEL fusion proteins. A probe containing the ABRE binding site motif was biotin-labeled and used in the reaction. The arrow indicates the EEL protein and ABRE probe complex.

SUPPLEMENTARY REFERENCES

Heidari P, Ahmadizadeh M, Najafi-Zarrini H. (2015) In Silico Analysis of Cis-Regulatory Elements on Co-Expressed Genes. J. Biol. Environ. Sci. 9(25):1-9.